53BP2 induces apoptosis through the mitochondrial death pathway

Shinya Kobayashi[1,2,†], Shinichi Kajino[1,2,†], Naoko Takahashi[1], Satoshi Kanazawa[1], Kenichi Imai[1], Yurina Hibi[1], Hirotaka Ohara[2], Makoto Itoh[2] and Takashi Okamoto[1,*]

[1]*Department of Molecular and Cellular Biology, and* [2]*Department of Internal Medicine and Bioregulation, Nagoya City University Graduate School of Medical Sciences, 1 Kawasumi, Mizuho-cho, Mizuho-ku, Nagoya, Aichi 467-8601, Japan*

The p53 binding protein 2 (53BP2) has been identified as the interacting protein to p53, Bcl-2, and p65 subunit of nuclear factor κB (NF-κB). The TP53BP2 gene encodes two splicing variants, 53BP2S and 53BP2L, previously known as apoptosis stimulating protein 2 of p53 (ASPP2). We found that these 53BP2 proteins are located predominantly in the cytoplasm and induce apoptosis as demonstrated by cleavage of poly ADP ribose polymerase (PARP) and annexinV staining. Furthermore, we demonstrate that 53BP2 is located in the mitochondria and induces apoptosis associated with depression of the mitochondrial trans-membrane potential ($\Delta\Psi m$) and activation of caspase-9. From these findings we conclude that 53BP2 induces apoptosis through the mitochondrial death pathway.

Introduction

Apoptosis is a well-defined biochemical pathway and is essential for the maintenance of cellular homeostasis in metazoans. Accumulating evidences indicate that the normal apoptotic pathway is affected in the pathological processes such as cancer and autoimmunity (Fisher *et al.* 1995; Green & Reed 1998; Jackson & Puck 1999; Daniel & Korsmeyer 2004). The induction of apoptosis occurs through two distinct pathways, the one elicited by death receptors in the plasma membrane ('extrinsic pathway') and the other directly involving mitochondria ('intrinsic pathway'). Whereas the former primarily involves activation of caspase-8, the latter apoptosis pathway is associated with the release of cytochrome C from mitochondria and activation of caspase-9 (for a review see Judith *et al.* 2004).

The p53 binding protein 2 (53BP2) has been initially identified as an interacting protein to p53 (Iwabuchi *et al.* 1994) and implicated in the biological action of p53. It was also shown that the 53BP2 binding site in the p53 core domain is evolutionarily conserved and is frequently mutated in human cancer (Iwabuchi *et al.* 1994; Gorina & Pavletich 1996). The subsequent studies have revealed that it interacts with Bcl-2 (Naumovski & Cleary 1996) and p65 subunit of nuclear factor κB (NF-κB) (Yang *et al.* 1999). Interestingly, 53BP2 has been shown to induce apoptosis (Yang *et al.* 1999), which was confirmed by others (Lopez *et al.* 2000; Ao *et al.* 2001; Samuels-Lev *et al.* 2001; Bergamaschi *et al.* 2004). However, the mechanism by which 53BP2 induces apoptosis has not been clarified.

53BP2 protein is encoded by a single copy gene *TP53BP2* located in the long arm of chromosome 1 at q42.1 (Yang *et al.* 1997). We have recently found that it encodes two distinct mRNA species, either with or without exon 3, by alternative splicing (Takahashi *et al.* 2004) (Fig. 1A). These splicing variants encode two 53BP2 proteins containing 1005 and 1128 amino acids (aa) with the longer isoform containing additional 123 amino acids in the N-terminus where no known functional motif or distinct intracellular localization signal is found. Although Samuels-Lev *et al.* (2001) renamed the longer 53BP2 isoform as ASPP2 (apoptosis stimulating protein of p53 2), we have proposed to call these proteins as 53BP2S (short) and 53BP2L (long) based on the genome organization of *TP53BP2* transcripts (Takahashi *et al.* 2004). 53BP2 proteins contain several structural and functional motifs including Gln-rich α-helical region, Pro-rich regions, ankyrin repeats, and Src-homology 3 domain.

Communicated by: Masayuki M. Yamamoto
**Correspondence*: E-mail: tokamoto@med.nagoya-cu.ac.jp
†These two authors contributed equally to this work.

DOI: 10.1111/j.1365-2443.2005.00835.x

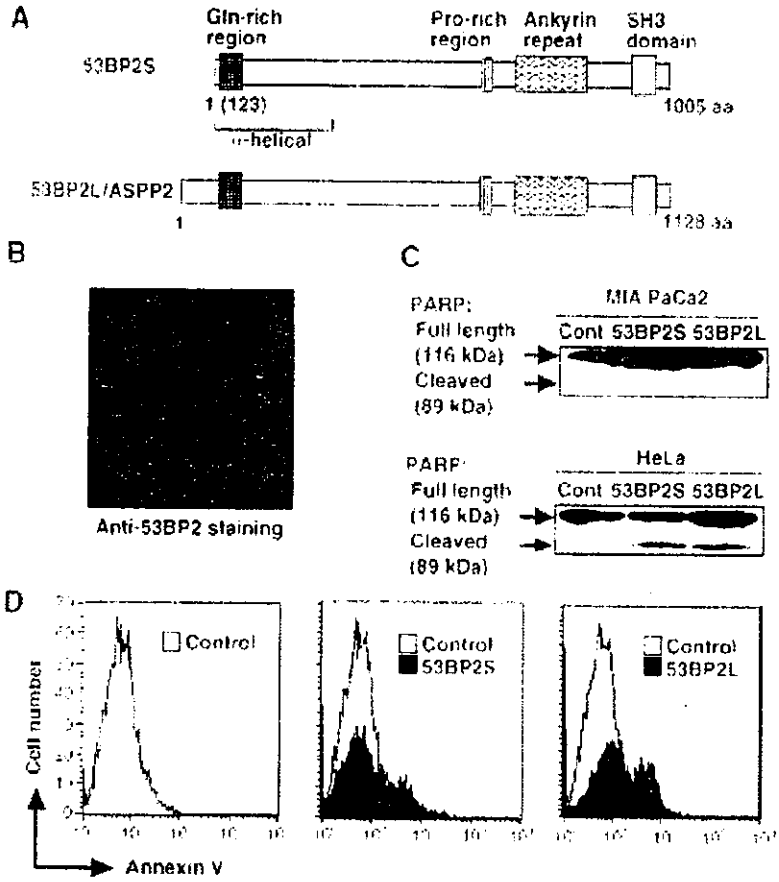

Figure 1 Induction of apoptosis by 53BP2 proteins. (A) Diagrammatic representation of 53BP2S and 53BP2L/ASPP2 proteins. Locations of Gln-rich region, putative 'α-helical region,' Pro-rich region, ankyrin repeats, and SH3 domain are indicated. Two splicing variants, 53BP2S and 53BP2L/ASPP2, containing 1005 amino acids and 1128 amino acids residues, respectively, are encoded by the same gene *TP53BP2* (Takahashi *et al.* 2004). 53BP2L contains additional 123 amino acid N-terminal region containing no apparent functional/structural motifs. (B) The localization of endogenous 53BP2 proteins in MIA PaCa-2 cells. Subcellular localization of endogenous 53BP2 was examined by immunostaining with anti-53BP2 mouse monoclonal antibody. The dim staining of 53BP2 proteins was repeatedly observed, which is presumably due to the low protein stability as previously indicated (Yang *et al.* 1999; Lopez *et al.* 2000). (C) Cleavage of PARP by 53BP2 proteins. MIA PaCa-2 cells and HeLa cells were transfected with pcDNA3.1–53BP2 ('53BP2S') or pCEP4–ASPP2 ('53BP2L') plasmids and the cell lysates were immunoblotted with anti-PARP antibody. The intact form of PARP (116 kDa) and its cleavage form (89 kDa) were detected by an anti-PARP rabbit polyclonal antibody (indicated by arrows). Note that no significant difference of the amounts of the cleaved form of PARP was found in cells expressing 53BP2S and 53BP2L. Cont, cells transfected with a control expression vector pcDNA3.1. (D) Induction of apoptosis by over-expression of 53BP2 proteins. MIA PaCa-2 cells were transfected with pcDNA3.1–53BP2 or pCEP4–ASPP2 and cells undergoing apoptosis were detected by flow cytometry. Live and dead cells were discriminated on the basis of their forward and side light-scattering properties. In order to evaluate cells undergoing apoptosis, cells were stained by both annexin V-PE and 7-AAD and those cells expressing 7-AAD were excluded from the measurement. The transfection efficiency was estimated to be approximately 65% by the GFP expression from the co-transfected pEGFP plasmid. The experiments were repeated more than three times with the same results.

In this study, we demonstrate that two 53BP2 isoforms, 53BP2S (previously called '53BP2') and 53BP2L ('ASPP2'), are localized predominantly in the cytoplasm and similarly induce apoptosis. We found that the mitochondrial death pathway is involved in the 53BP2-mediated apoptosis. The biological roles of 53BP2 and its interacting proteins in the regulation of apoptosis are discussed.

Results

Induction of apoptosis by 53BP2 proteins

Figure 1A illustrates the organization of 53BP2 isoforms as previously reported (Takahashi *et al.* 2004). As shown in Fig. 1B, the endogenous 53BP2 proteins were localized predominantly in the cytoplasm, confirming the previous reports wherein 53BP2 was over-expressed (Iwabuchi *et al.* 1998; Yang *et al.* 1999). To compare the effect of 53BP2S and 53BP2L, these proteins were transduced in MIA PaCa-2 and HeLa cells. After 48 h of transfection, the cleaved form of poly ADP ribose polymerase (PARP; 89 kDa product), a hallmark of apoptosis, was detected (Fig. 1C). When 53BP2S and 53BP2L were over-expressed in MIA PaCa-2 cells, approximately 16% and 27% of cells were found undergoing early apoptotic process (annexin V (+), 7-AAD (–)), respectively, whereas the percentage of apoptotic cells in the control was only 1.8% (Fig. 1D). The extents of apoptosis were similar to our previous observations using various DNA damaging agents (Mori *et al.* 2000).

Induction of apoptosis in a stable transfectant (293/53BP2)

We then examined the action of 53BP2 using the 293/53BP2 cells, in which expression of 53BP2S is under stringent control by ponasteron A (pon A). In Fig. 2A, both 293/53BP2 and its control 293/LZ were treated with pon A. The 53BP2S protein became detectable after 12 h of induction by pon A (5 μM) in a time-dependent manner and induced apoptosis as early as 24 h after pon A treatment. As shown in Fig. 2B, after 72 h of 53BP2S expression, a significant number (26%) of cells underwent apoptosis as revealed by positive staining for annexin V, whereas only the background level (6.5%) was stained in control cells. Cells at early apoptotic process (annexin (+), 7-AAD (–)) were found 14% and 3% in 293/53BP2 cells and control cells, respectively (Fig. 2B). No cleavage of PARP or a significant annexin V staining was detected with the control 293/LZ cells (data not shown).

Cytosolic and mitochondrial localization of 53BP2S

In Fig. 3A, intracellular localization of 53BP2S was examined by transfection of pEGFP53BP2 expressing 53BP2S in fusion with green fluorescence protein (GFP). A punctate vesicular pattern was noted, localized predominantly in the cytoplasm of the transfected cells. To confirm the localization of 53BP2S, we co-transfected pDsRed2-Mito, expressing red fluorescent protein targeted to mitochondria. As demonstrated in Fig. 3A and

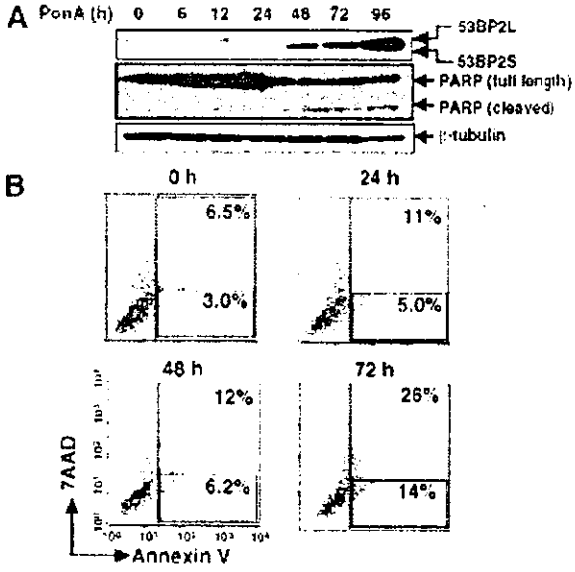

Figure 2 Induction of apoptosis in 293/53BP2 cell line. (A) Time course of induction of 53BP2S and cleavage of PARP in 293/53BP2 cells. Cells were treated with pon A (5 μM) using an ecdysone-inducible expression system for the indicated periods (h), and the cell lysate (10 μg protein) was examined for the expression of 53BP2S and PARP. The intact full-length PARP (116 kDa) was cleaved into 89 kDa during the apoptotic process. Longer exposure of chemiluminescence for protein detection revealed the endogenous 53BP2L protein in these cells. β-tubulin was used as an internal control. (B) Flow cytometric detection of apoptotic cells. 293/53BP2 cells were stimulated with pon A (5 μM) and cultured for the indicated periods (h). The percentages of cells at apoptosis (annexin V (+)) and cells at early apoptosis (annexin V positive and 7-AAD (–)) were counted and indicated separately.

53BP2S was shown to be partly localized in the mitochondria in addition to the cytoplasm. In most cells only portions of mitochondria were costained with 53BP2S, suggesting that small amounts of 53BP2S molecules could be sufficient to induce apoptosis. In Fig. 3B, subcellular fractionation was performed and the presence of 53BP2S was examined. Protein expression was induced by pon A for 48 h and each subcellular fraction was subjected to Western blotting with anti-53BP2 antibody. Although majority of the 53BP2S protein was detected in the cytosolic fraction, it was also detected in the mitochondrial fraction (Fig. 3B).

Depression of $\Delta\Psi$m by 53BP2S expression

These findings suggested the involvement of the 'intrinsic' death pathway. We thus examined the change in $\Delta\Psi$m

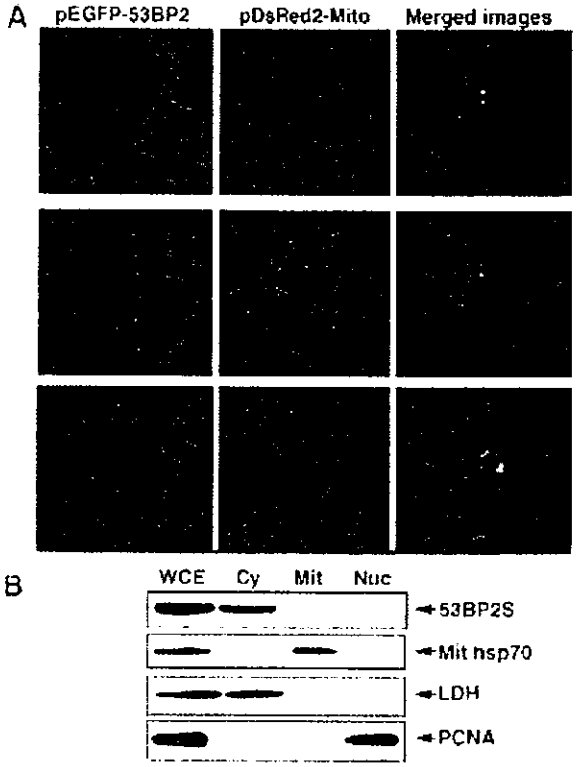

Figure 3 Intracellular localization of 53BP2S. (A) Co-localization of 53BPS and mitochondria marker. 293 cells were transiently transfected with pEGFP-53BP2 and mitochondria-targeting plasmid pDsRed2-Mit and examined under confocal microscope. The GFP fluorescence, DsRed fluorescence and merged images of cells are shown. Note that only portions of mitochondria (visualized by DsRed) were costained with GFP (53BP2S). (B) Subcellular fractionation. Upon induction of 53BP2 by pon A (5 μM, 48 h) in 293/53BP2 cells, whole cell extract (WCE) was prepared. The cytoplasmic (Cy), mitochondrial (Mit) and nuclear (Nuc) fractions were separated as described in Experimental procedures. Each protein fraction was separated by 10% SDS-PAGE, and probed with antibodies to 53BP2S, PCNA (nuclear marker), mitochondrial heat shock protein (Mit hsp70) and LDH (cytoplasmic marker). The same cell equivalents were loaded on each lane. Contamination of the cytoplasmic fraction into the mitochondria fraction was considered negligible because of the absence of LDH. The identical results were obtained repeatedly.

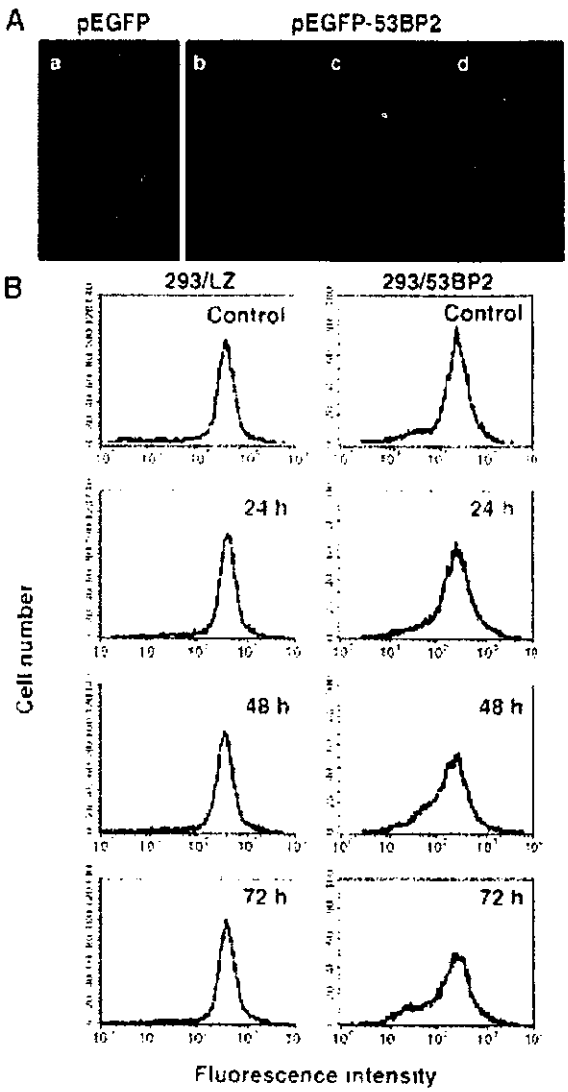

Figure 4 Alteration of the mitochondria transmembrane potential ($\Delta\Psi m$) by 53BP2S. (A) Reduction of $\Delta\Psi m$ by 53BP2S. After 48 h of transfection with pEGFP (a) or pEGFP53BP2 (b–d) plasmids, MIA PaCa-2 cells were stained with CMXRos. Typical cells are shown. In cells expressing 53BP2S, progressive reduction of $\Delta\Psi m$ was observed in association with nuclear fragmentation (from b–d). The same exposure time was used in each picture. (B) Temporal change of $\Delta\Psi m$ following 53BP2S induction. 293/53BP2 and 293/LZ cells were treated with pon A for indicated periods (h), stained with rhodamine 123, and flow cytometric analysis was performed. Distribution of fluorescence intensity of cells with sham treatment (only the solvent ethanol was added) is shown in gray shadow. 'Control,' uninduced cells.

following 53BP2S expression (Fig. 4). Several cationic, lipophilic, fluorescent dyes such as CMXRos and rhodamine 123, can readily detect changes in $\Delta\Psi m$ as they are selectively sequestered by respiring mitochondria by virtue of their negative charges on the inner membrane and are washed out when $\Delta\Psi m$ is lost. As shown in Fig. 4A, the extent of CMXRos staining in pEGFP53BP2-transfected cells (visualized by the expression of GFP)

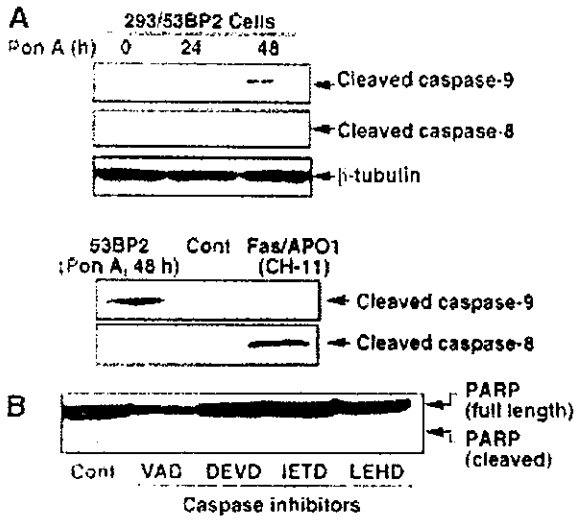

Figure 5 Involvement of caspase-9 in apoptosis induced by 53BP2S. (A) Activation of caspase-9 by 53BP2S. 293/53BP2 cells were treated by pon A (5 μM) for the indicated periods (h). Each cell lysate (10 μg protein) was examined for the activated ('cleaved') form of caspase-9 by Western blotting with anti-caspase-9 (cleaved form) or anti-caspase-8 (cleaved form) antibodies (upper panel). β-tubulin was used as an internal control. In the lower panel, 293/53BP2 cells were either stimulated with the agonistic anti-Fas antibody (CH-11) or treated with pon A and the activation of caspase-8 or caspase-9 was similarly examined. (B) Inhibition of the PARP cleavage by caspase inhibitors. 293/53BP2 cells were cultured with or without caspase inhibitors for 12 h and treated with pon A (5 μM) for 48 h. The cell lysate was prepared and examined for the PARP cleavage by Western blotting. The same amounts of each cell lysate (10 μg protein) were analyzed. Cont, DMSO alone; VAD, common inhibitor for the caspase-family (Z-VAD-FMK); DEVD, caspase-3-specific inhibitor (Z-DEVD-FMK); IETD, caspase-8-specific inhibitor (Z-IETD-FMK); LEHD, caspase-9-specific inhibitor (Z-IETD-FMK).

was diminished, indicating a decrease in $\Delta\Psi m$. In contrast, no such changes were observed in the control cells transfected with pEGFP. In Fig. 4B, the temporal change of $\Delta\Psi m$ in 293/53BP2 cells is shown. When 53BP2S was expressed, progressive reduction of $\Delta\Psi m$ detected by the rhodamine123 fluorescence intensity was observed over time, concomitantly with the appearance of apoptotic cells (compare with Fig. 2B). No such change was observed in control 293/LZ cells.

Involvement of caspase-9 in apoptosis induced by 53BP2S

Finally, to examine the upstream caspase cascade involved in the 53BP2S-mediated apoptosis, 293/53BP2 cell lysates were prepared after 24 and 48 h of pon A treatment. The presence of activated (cleaved) forms of caspase-8 and caspase-9 were examined in these cells. Figure 5A shows that caspase-9, but not caspase-8, was activated following the induction of 53BP2S. To confirm these observations, the effects of specific inhibitors for caspase-3, -8, and -9 were examined. As shown in Fig. 5B, the effects of peptide inhibitors among all types of known caspases (VAD), caspase-3 (DEVD), caspase-8 (IETD) and caspase-9 (LEHD) were shown. Although VAD, DEVD and LEHD effectively blocked the PARP cleavage induced by 53BP2S, only a minimal effect was observed with IETD. These findings indicate that 53BP2S induces apoptosis through the mitochondrial ('intrinsic') death pathway.

Discussion

The present data have revealed the involvement of mitochondria in the 53BP2-mediated apoptosis. 53BP2 has two protein isoforms, 53BP2S and 53BP2L, generated by alternative splicing (Takahashi *et al.* 2004). These two 53BP2 proteins are localized predominantly in the cytoplasm and exhibited similar biological actions although we do not currently know the reason of such redundancy. In this study, we have explored the proapoptotic action of 53BP2S using transient expression and the stable cell line in which 53BP2 is under the stringent control of pon A. When expressed, 53BP2S was located in the mitochondria and induced cell death associated with $\Delta\Psi m$ repression, caspase-9 activation, PARP cleavage, annexinV staining, and typical nuclear morphology, suggesting the involvement of intrinsic death pathway.

Regarding the possible involvement of 53BP2 in the cellular response to DNA damage, we have previously reported the positive correlation between the level of 53BP2 mRNA expression and the sensitivity to DNA damaging agents in various human cancer cell lines although no mutation of 53BP2 gene was detected (Mori *et al.* 2000). In addition, Ao *et al.* (2001) found that 53BP2S expression augmented the cellular apoptotic response to the DNA damage. Lopez *et al.* (2000) observed that the DNA damage induced the 53BP2 expression and protein stabilization leading to apoptosis. Bergamaschi *et al.* (2004) recently reported similar observations with ASPP2 (53BP2L). Therefore, it is likely that the activated p53 may augment the 53BP2-mediated cell death. In support of this action of p53, Marchenko *et al.* (2000) demonstrated the mitochondrial translocation of p53 upon irradiation and induction of apoptosis through the intrinsic death pathway. Mihara *et al.* (2003) further explored the mitochondrial involvement of p53 and found that p53 formed a complex with

Bcl-2 and $BclX_L$ followed by permeabilization of the outer mitochondrial membrane.

Intriguingly, Iwabuchi *et al.* (1998) and Samuels-Lev *et al.* (2001) found that p53-mediated transactivation was augmented by 53BP2S and 53BP2L (ASPP2), respectively. Samuels-Lev *et al.* (2001) proposed a model that 53BP2L interacts with p53 in the nucleus and specifically enhances gene expression of p53 responsive pro-apoptotic genes such as Bax. Although the 3D structure model of p53 and 53BP2 complex (Gorina & Pavletich 1996) does not support their hypothesis because when 53BP2 binds to p53, it involves the L3 loop of p53 (required for its DNA binding) and the H1 helix (required for p53 dimerization), thus precluding the p53 binding to DNA, there may be multiple mechanisms by which 53BP2 induces apoptosis.

In addition to the possible involvement of p53 and 53BP2 in apoptosis, 53BP2 abnormality is implicated in autoimmunity such as systemic lupus erythematosus (SLE) since one of the genetic loci of the familial incidence of SLE was shown to be located to 1q42.1 (Tsao *et al.* 1997), to which *TP53BP2* is located (Yang *et al.* 1997). This is coincided with the fact that abnormalities of various apoptosis-associated factors were reported in SLE and its animal models (Fisher *et al.* 1995; Sneller *et al.* 1997; Jackson & Puck 1999). Further genetic studies are needed to find a link between 53BP2 and autoimmunity.

Our observations together with those of others suggest that 53BP2 is involved in apoptosis at multiple steps and is implicated in various pathological processes. Since 53BP2 has been shown to interact with a number of proteins responsible for the regulation of apoptosis such as p53, Bcl-2 and NF-κB p65 subunit, selective interaction of 53BP2 with these proteins may determine the susceptibility of cells to trigger the apoptotic pathway.

Experimental procedures

Reagents and antibodies

FuGENE 6 and SuperFect transfection reagents were purchased from Roche Molecular Biochemicals (Indianapolis, IN, USA) and QIAGEN (Qiagen Inc., Valencia, CA, USA), respectively. PE-conjugated annexin V and 7-AAD (Becton Dickenson, Mountain View, CA, USA), ponasterone A (pon A) (Invitrogen, La Jolla, CA, USA) were commercially obtained. The caspase inhibitors (caspase-3 inhibitor, Z-DEVD-FMK; caspase-8 inhibitor, Z-IETD-FMK; caspase-9 inhibitor, Z-LEHD-FMK; caspase-family inhibitor, Z-VAD-FMK) were purchased from MBL. Mouse monoclonal antibodies to human 53BP2 (BD Transduction Laboratories, San Diego, CA, USA), β-tubulin (Sigma Chemical Co., St. Louis, MO, USA), human lactate dehydrogenase (LDH) (MBL, Nagoya, Japan) and human Fas (Sigma), and mouse polyclonal antibody to human mitochondrial heat shock protein 70 (Affinity Bioreagents, Golden, CO, USA) were purchased from individual suppliers. The rabbit polyclonal antibody to human 53BP2 was a generous gift from L. Naumovski (Stanford University, CA, USA). Mouse monoclonal antibodies to caspase-8 (cleaved form) and caspase-9 (cleaved form) and rabbit polyclonal antibody to PARP were purchased from Cell Signaling Technology (Beverly, MA, USA).

Plasmids

Construction of the 53BP2S expression plasmids, pcDNA3.1–53BP2 and pEGFP-53BP2, expressing 53BP2S protein (1005 amino acids) either alone or in fusion with green fluorescence protein (GFP), was reported previously (Yang *et al.* 1999). pCEP4-ASPP2, expressing 53BP2L (1128 amino acids), was a gift from L. Naumovski. pDsRed2-Mito, expressing a fusion protein of the *Discosoma* sp. red fluorescent protein linked to the mitochondrial targeting sequence from subunit VIII of human cytochrome oxidase, was purchased from BD Bioscience Clontech (Palo Alto, CA, USA).

Cell lines and cultures

The 53BP2S inducible cell line 293/53BP2 and its control cell line 293/LZ were kindly provided by Charles D. Lopez, Stanford University, CA, USA and previously described (Lopez *et al.* 2000). These cells were grown at 37 °C in 5% CO_2 in Dulbecco's modified Eagle medium (DMEM) with 10% (v/v) heat-inactivated foetal calf serum, 290 μg/mL of L-glutamine, 100 U/mL penicillin, 100 μg/mL streptomycin, 600 μg/mL G418 and 500 μg/mL Zeocin. The parental 293 and HeLa cells were grown at 37 °C in DMEM with 10% (v/v) heat-inactivated foetal calf serum (IBL, Maebashi, Japan), 1 mM glutamate, 100 U/mL penicillin, and 100 μg/mL streptomycin. A human pancreatic cancer cell line MIA PaCa-2 was grown in Eagle minimal essential medium supplemented with nonessential amino acids, 10% (v/v) heat-inactivated foetal calf serum, 100 U/mL penicillin, and 100 μg/mL streptomycin.

Immunostaining

Semi-confluent MIA PaCa-2 cells on Laboratory-Tek tissue culture chamber slides were fixed with 4.5%

paraformaldehyde in PBS for 15 min at room temperature, rinsed twice with PBS, and incubated with PBS containing 0.5% Triton X-100 for 20 min at room temperature. They were subsequently incubated with the primary anti-53BP2 mouse antibody (B92320, Transduction Laboratories, Lexington, KY, USA) for 1 h at 37 °C, rinsed three times with PBS containing 0.05% Triton X-100, and incubated with the secondary antibody, rhodamine-conjugated goat anti-mouse IgG (Calbiochem-Novabiochem, La Jolla, CA, USA), for 1 h at 37 °C. The slides were rinsed with PBS three times and mounted with buffered glycerol for fluorescent microscopic examination. Primary and secondary antibodies were diluted at 1 : 100 and 1 : 200, respectively, in PBS containing 3% bovine serum albumin.

Cell fractionation

In order to examine the cellular localization of 53BP2 in the 293/53BP2 cells, cells were pretreated with pon A (5 μM, 48 h) and subjected to fractionation using commercial kits (Nuclear/Cytosol Fractionation Kit and Mitochondria/Cytosol Fractionation Kit, BioVision, Mountain View, CA, USA). The heavy membrane precipitate containing mitochondria was extensively washed in order to avoid the contamination of cytoplasmic proteins. The identification of 53BP2 and validation of cell fractionation were performed by Western blotting with antibodies to 53BP2, LDH (cytoplasmic marker) and mitochondrial heat shock protein 70 (mitochondria marker).

Flow cytometric analysis of apoptosis

In order to assess apoptosis, flow cytometric analysis was performed using FACScan (Becton Dickinson). MIA PaCa-2 cells were transiently transfected with pcDNA3.1–53BP2 expressing 53BP2S or pCEP4-ASPP2 expressing 53BP2L using SuperFect according to the manufacturer's recommendations. Cells at a concentration of approximately 1×10^6 cells/mL were washed twice with cold PBS and resuspended in annexin V binding buffer (10 mM HEPES-NaOH (pH 7.4), 140 mM NaCl and 2.5 mM $CaCl_2$). In some experiments, cells were double-stained with annexin V and 7-Amino-actinomycin D (7-AAD). 293/53BP2 cells were induced to express 53BP2 by incubation with 5 μM pon A and apoptotic cells were similarly counted.

Microscopic examination

In order to examine the cellular localization of 53BP2S, 293 cells were cultured on 2-well Laboratory-Tek tissue culture chamber slides and transfected with 0.4 μg of pEGFP-53BP2 expressing 53BP2S together with 0.1 μg of the mitochondria targeting plasmid, pDsRed2-Mito (BD Bioscience Clontech). The transfected cells were fixed with 4.0% paraformaldehyde in PBS for 15 min at room temperature, and observed under the confocal microscope (RADIANCE2000; Bio-Rad, Hercules, CA, USA). Each fluorophore was recorded separately using narrow-band filters centered at 522 nm for GFP fluorescence and 605 nm for DsRed2 fluorescence.

Evaluation of apoptosis by Western blotting

Apoptosis was also assessed by the cleavage of PARP, and caspases-8 and -9 by Western blotting using relevant antibodies described above. Briefly, whole cell extracts were lyzed in 200 μL of ice-cold lysis buffer (50 mM Tris-HCl (pH 8.0), 100 mM NaCl, 5 mM EDTA, 50 mM sodium fluoride, 2 mM dithiothreitol, 0.25% Nonidet P-40, 1 mM phenylmethyl-sulfonyl fluoride, 10 μg/mL aprotinin, 10 μg/mL leupeptin and 1 μg/mL pepstatin (A). The lysate was cleared by centrifugation and the protein concentration of the whole cell extract was measured using Bio-Rad DC protein assay kit (Bio-Rad). Equal amounts of cell lysates (10 μg protein) were resolved by 10% SDS-PAGE and transferred on nitrocellulose membrane followed by incubating with individual antibodies. The immunoreactive proteins were visualized by ECL.

Determination of mitochondrial $\Delta\Psi m$ in cultured cells

To evaluate $\Delta\Psi m$, cells were treated with 10 μg/mL Rh123 for 15 min at 37 °C. After incubation, cells were washed with PBS(+) three times, resuspended in PBS(+), and fluorescence was scored immediately by flow cytometer. To visualize the cells with depressed $\Delta\Psi m$, cells growing on Laboratory-*Tek*II chambered cover glass were stained with 40 nM CMXRos in PBS(+) for 15 min, washed with PBS(+) three times and observed under the confocal microscope (Bio-Rad MRC600UVF). The acquisitions of the mitochondrial images were provided by 585LP emission filter with same setting (Iris: 2.0, Gain: 1.4).

Acknowledgments

We thank Dr Louie Naumovski (Stanford University) for his generous gifts of 293/53BP2 cells, polyclonal antibody to 53BP2, and a plasmid expressing 53BP2L. This work was supported in part by grants-in-aid from the Ministry of Health, Labor and Welfare, the

Ministry of Education, Culture, Sports, Science and Technology of Japan and Japanese Human Sciences Foundation.

References

Ao, Y., Rohde, L.H. & Naumovski, L. (2001) p53-interacting protein 53BP2 inhibits clonogenic survival and sensitizes cells to doxorubicin but not paclitaxel-induced apoptosis. *Oncogene* **20**, 2720–2725.

Bergamaschi, D., Samuels, Y., Jin, B., Duraisingham, S., Crook, T. & Lu, X. (2004) ASPP1 and ASPP2: Common activators of p53 family members. *Mol. Cell. Biol.* **24**, 1341–1350.

Daniel, N.N. & Korsmeyer, S.J. (2004) Cell death: Critical control points. *Cell* **116**, 205–219.

Fisher, G.H., Rosenberg, F.J., Straus, S.E., *et al.* (1995) Dominant interfering Fas gene mutations impair apoptosis in a human autoimmune lymphoproliferative syndrome. *Cell* **81**, 935–946.

Gorina, S. & Pavletich, N.P. (1996) Structure of the p53 tumor suppressor bound to the ankyrin and SH3 domains of 53BP2. *Science* **274**, 1001–1005.

Green, D.R. & Reed, J.C. (1998) Mitochondria and apoptosis. *Science* **281**, 1309–1312.

Iwabuchi, K., Bartel, P.L., Li, B., Marraccino, R. & Fields, S. (1994) Two cellular proteins that bind to wild-type but not mutant p53. *Proc. Natl. Acad. Sci. USA* **91**, 6098–6102.

Iwabuchi, K., Li, B., Massa, H.F., Trask, B.J., Date, T. & Fields, S. (1998) Stimulation of p53-meditated transcriptional activation by the p53-binding proteins, 53BP1 and 53BP2. *J. Biol. Chem.* **273**, 26061–26068.

Jackson, C.E. & Puck, J.M. (1999) Autoimmune lymphoproliferative sundrome, a disorder of apoptosis. *Curr. Opin. Pediatr.* **11**, 521–527.

Judith, H.M., Caroline, D., Jean, C.M. & James, D. (2004) Role of mitochondrial membrane permeabilization in apoptosis and cancer. *Oncogene* **23**, 2850–2860.

Lopez, C.D., Ao, Y., Rohde, L.H., *et al.* (2000) Proapoptotic p53-interacting protein 53BP2 is induced by UV irradiation but suppressed by p53. *Mol. Cell. Biol.* **20**, 8018–8025.

Marchenko, N.D., Zaika, A. & Moll, U.M. (2000) Death signal-induced localization of p53 protein to mitochondria. A potential role in apoptotic signaling. *J. Biol. Chem.* **275**, 16202–16212.

Mihara, M., Erster, S., Zaika, A., *et al.* (2003) p53 has a direct apoptogenic role at the mitochondria. *Mol. Cell* **11**, 577–590.

Mori, T., Okamoto, H., Takahashi, N., Ueda, R. & Okamoto, T. (2000) Aberrant overexpression of 53BP2 mRNA in lung cancer cell lines. *FEBS Lett.* **465**, 124–128.

Naumovski, L. & Cleary, M.L. (1996) The p53-binding protein 53BP2 also interacts with Bc12 and impedes cell cycle progression at G2/M. *Mol. Cell. Biol.* **16**, 3884–3892.

Samuels-Lev, Y., O'Connor, D.J., Bergamaschi, D., *et al.* (2001) ASPP proteins specifically stimulate the apoptotic function of p53. *Mol. Cell* **8**, 781–794.

Sneller, M.C., Wang, J., Dale, J.K., *et al.* (1997) Clinical, immunologic, and genetic features of an autoimmune lymphoproliferative syndrome associated with abnormal lymphocyte apoptosis. *Blood* **89**, 1341–1348.

Takahashi, N., Kobayashi, S., Jiang, X., *et al.* (2004) Expression of 53BP2 and ASPP2 proteins from TP53BP2 gene by alternative splicing. *Biochem. Biophys. Res. Commun.* **315**, 434–438.

Tsao, B.P., Canto, R.M., Kaluuian, K.C., *et al.* (1997) Evidence for linkage of a candidate chromosome 1 region to human systemic lupus erythematosus. *J. Clin. Invest.* **99**, 725–731.

Yang, J.P., Ono, T., Sonta, S., Kawabe, T. & Okamoto, T. (1997) Assignment of p53 binding protein (TP53BP2) to human chromosome band 1q42.1 by in situ hybridization. *Cytogenet. Cell Genet.* **78**, 61–62.

Yang, J.P., Hori, M., Takahashi, N., Kawabe, T., Kato, H. & Okamoto, T. (1999) NF-κB subunit p65 binds to 53BP2 and inhibits cell death induced by 53BP2. *Oncogene* **18**, 5177–5186.

Received: 8 October 2004
Accepted: 12 December 2004

Eur. J. Biochem. 271, 3741–3751 (2004) © FEBS 2004 doi:10.1111/j.1432-1033.2004.04314.x

RNA helicase A interacts with nuclear factor κB p65 and functions as a transcriptional coactivator

Toshifumi Tetsuka[1], Hiroaki Uranishi[1], Takaomi Sanda[1], Kaori Asamitsu[1], Jiang-Ping Yang[2], Flossie Wong-Staal[2] and Takashi Okamoto[1]

[1]*Department of Molecular and Cellular Biology, Nagoya City University Graduate School of Medical Sciences, Nagoya, Aichi, Japan;* [2]*Department of Medicine, University of California San Diego, La Jolla, CA, USA*

RNA helicase A (RHA), a member of DNA and RNA helicase family containing ATPase activity, is involved in many steps of gene expression such as transcription and mRNA export. RHA has been reported to bind directly to the transcriptional coactivator, CREB-binding protein, and the tumor suppressor protein, BRCA1, and links them to RNA Polymerase II holoenzyme complex. Using yeast two-hybrid screening, we have identified RHA as an interacting molecule of the p65 subunit of nuclear factor κB (NF-κB). The interaction between p65 and RHA was confirmed by glutathione-*S* transferase pull-down assay *in vitro*, and by co-immunoprecipitation assay *in vivo*. In transient transfection assays, RHA enhanced NF-κB dependent reporter gene expression induced by p65, tumor necrosis factor-α, or NF-κB inducing kinase. The mutant form of RHA lacking ATP-binding activity inhibited NF-κB dependent reporter gene expression induced by these activators. Moreover, depletion of RHA using short interfering RNA reduced the NF-κB dependent transactivation. These data suggest that RHA is an essential component of the transactivation complex by mediating the transcriptional activity of NF-κB.

Keywords: coactivator; NF-κB; protein–protein interaction; RNA helicase A; transcription.

Nuclear factor κB (NF-κB) is an inducible cellular transcription factor that regulates a wide variety of cellular and viral genes including cytokines, cell adhesion molecules and HIV [1–3]. The members of the NF-κB family in mammalian cells include the proto-oncogene c-Rel, RelA (p65), RelB, NFkB1 (p50/105), and NFkB2 (p52/p100). In most cells, Rel family members form hetero- and homodimers with distinct specificities in various combinations. p65, RelB and c-Rel are transcriptionally active members of the NF-κB family, whereas p50 and p52 serve primarily as DNA binding subunits [1–3]. These proteins play fundamental roles in immune and inflammatory responses and in the control of cell proliferation [4,5]. A common feature of the regulation of NF-κB is their sequestration in the cytoplasm as an inactive complex with a class of inhibitory molecules known as IκBs. Treatment of cells with a variety of inducers such as interleukin-1 (IL-1) and tumor necrosis factor (TNF) results in phosphorylation, ubiquitination and degradation of the IκB proteins [1–3].

The protein regions responsible for the transcriptional activation [called 'transactivation (TA) domain'] of p65, Rel B and c-Rel have been mapped in their unique C-terminal regions. p65 contains at least two independent TA domains within its C-terminal 120 amino acids (Fig. 1A). One of these TA domains, TA1, is confined to the C-terminal 30 amino acids of p65. The second TA domain, TA2, is localized in the N-terminally adjacent 90 amino acids and contains TA1-like motif. As the nuclear translocation and DNA binding of NF-κB were not sufficient for gene induction [6,7], it was suggested that interactions with other protein molecules through the TA domain [8–10] as well as its modification by phosphorylation [11–14] might play critical roles in the NF-κB-mediated gene expression.

It has been shown that NF-κB requires multiple coactivator proteins including CREB-binding protein (CBP)/p300 [8–10,15,16], CBP associated factor, and steroid receptor coactivator 1 [17]. These proteins have histone acetyl transferase activity that modifies chromatin structure and provides molecular bridges to the basal transcriptional machinery. p65 was also found to interact with a newly identified coactivator complex, activator-recruited cofactor/vitaminD receptor-interacting protein, which potentiated chromatin-dependent transcriptional activation by NF-κB *in vitro* [18]. Aside from coactivators, the transcriptional activity of gene-specific activators can also be mediated by general transcription factors.

Correspondence to T. Okamoto, Department of Molecular and Cellular Biology, Nagoya City University Graduate School of Medical Sciences, 1 Kawasumi, Mizuho-cho, Mizuho-ku, Nagoya, Aichi 467–8601, Japan. Fax: +81 52 859 1235, Tel.: +81 52 853 8204, E-mail: tokamoto@med.nagoya-cu.ac.jp

Abbreviations: AD, (transcriptional) activation domain; AES, amino-terminal enhancer of split; CREB, cAMP response element binding protein; CBP, CREB-binding protein; CMV, cytomegalovirus; DBD, DNA-binding domain; GIR, Groucho-interacting region; Grg, Groucho-related genes; GST, glutathione-*S* transferase; ICAM-1, intercellular adhesion molecule-1; IFN-β, interferon-β; IL-1, interleukin-1; MLE, maleless; MSL, male-specific lethal; NF-κB, nuclear factor κB; NIK, NF-κB inducing kinase; NLS, nuclear localization signal; RAI, RelA-associated inhibitor; RHA, RNA helicase A; RNA Pol II, RNA polymerase II; TLE1, transducin-like enhancer of split 1; TLS, translocated in liposarcoma; TNF-α, tumor necrosis factor-α.

(Received 8 April 2004, revised 15 July 2004, accepted 30 July 2004)

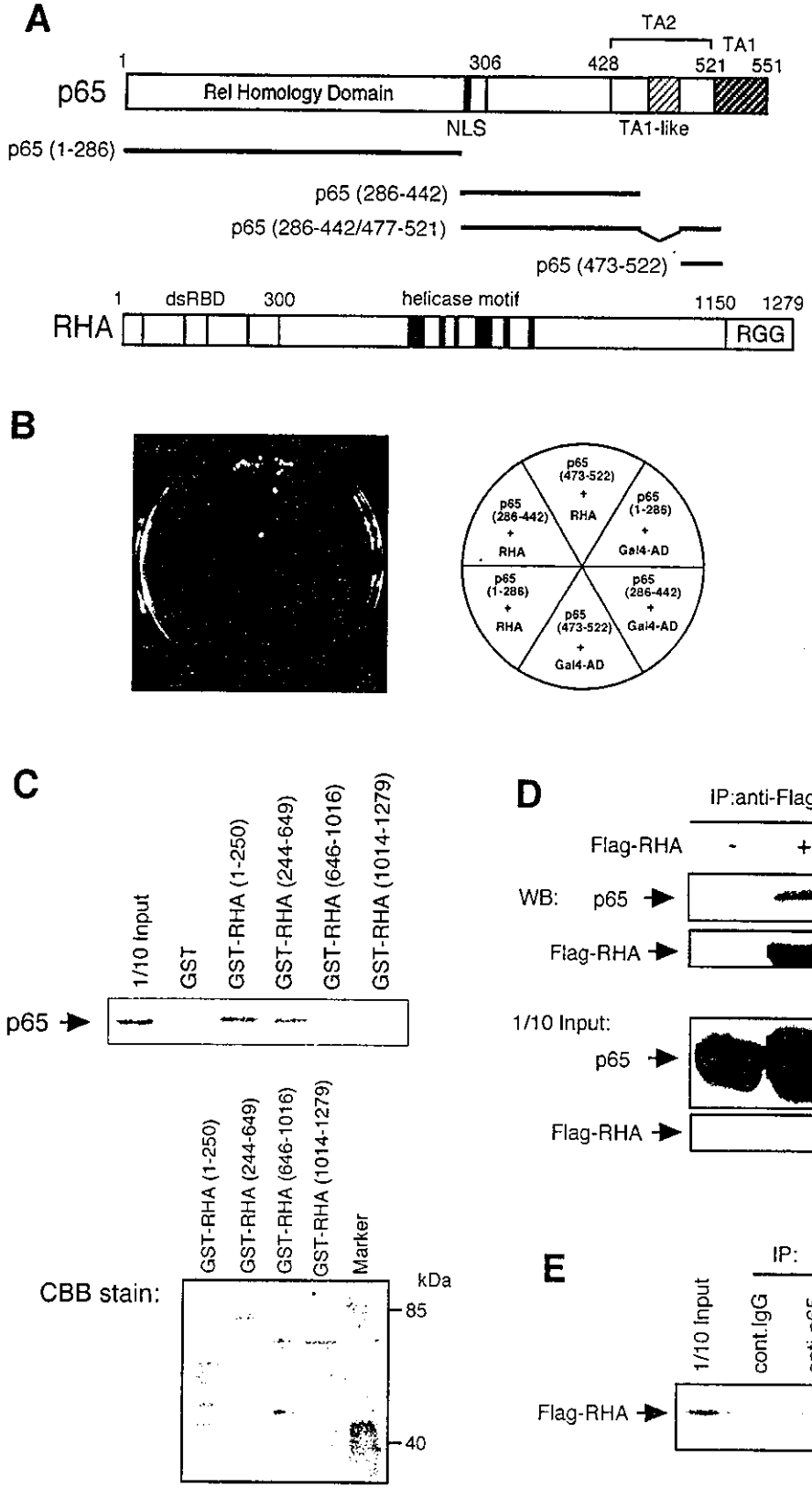

In the case of NF-κB, the association of p65 with general transcription factors such as TFIIB, $TAF_{II}105$, and TBP has been demonstrated [8,19–22]. It is thus postulated that specific protein–protein interactions with NF-κB determine its transcriptional competence. Up-regulation of the NF-κB transcriptional activity is mediated by interaction with basal factors and coactivators while its down-regulation is mediated by interaction with inhibitors and corepressors at

Fig. 1. Interaction between p65 and RHA. (A) Schematic illustrations of various functional domains of p65 and RHA. dsRBD, double stranded RNA-binding domain; NLS, nuclear localization signal; TA1, transactivation domain 1; TA2, transactivation domain 2 (containing TA1-like domain, Groucho-interacting region, and leucine-rich region); RGG, Arg-Gly-Gly rich region. (B) Growth of yeast transformants coexpressing p65 and RHA on the selective medium. The yeast Y190 was transformed with pACT2-RHA and pGBT plasmids expressing various portions of the p65 in fusion with Gal4-DBD. The yeast transformants grown on plates lacking Leu and Trp were streaked on plates lacking Leu, Trp and His, and containing 25 mM 3-aminotriazole. (C) p65 binds to RHA *in vitro*. p65 was labeled with [^{35}S]-methionine by *in vitro* transcription/translation. Radiolabeled p65 was incubated with GST, GST-RHA(1–250), GST-RHA(244–649), GST-RHA(646–1016) or GST-RHA(1014–1279) immobilized on glutathione-Sepharose beads. After incubation and further washing, the complexes were resolved by 10% SDS/PAGE and subjected to autoradiography. (D,E) p65 binds to RHA *in vivo*. HEK 293 cells were transfected with pCMV-p65 in combination with either pCMV-Flag-RHA or the empty vector. Whole cell extracts were harvested 48 h after transfection, and immunoprecipitated with 10 μL of anti-Flag M2 Affinity Gel, and the resulting precipitates were disrupted and immunoblotted with anti-p65 Ig and anti-Flag Ig (D, upper panel). Whole cell extracts (1/10 input) were also immunoblotted with anti-p65 Ig and anti-Flag Ig to show that the same amount of the immune complex containing p65 were loaded (D, lower panel). HEK 293 cells were transfected with pCMV-Flag-RHA and pCMV-p65 expression vectors. Whole cell extract was harvested 48 h after transfection, and RHA was immunoprecipitated with control rabbit IgG or anti-p65 rabbit polyclonal IgG. Ten microliters of protein G-agarose beads was added and the reaction was further incubated for 1 h. The immunoprecipitated proteins were resolved by 10% SDS/PAGE and immunoblotted with anti-Flag Ig (E).

multiple levels. In our previous studies, yeast two-hybrid screening yielded several novel regulators of NF-κB that interact with the p65 subunit: amino-terminal enhancer of split (AES) and transducin-like enhancer of split (TLE1) [23], both belonging to the Groucho-related genes (Grg) and acting as corepressors. The pro-oncoprotein TLS (translocated in liposarcoma), a homologue of $TAF_{II}68$, stimulates the transcriptional activity of p65 [24]. These proteins interact with a small intervening region between TA1 and TA1-like motifs, termed 'Groucho-interacting region' (GIR), within the C-terminal TA domain of p65 [23,24]. In addition, we also identified a novel nuclear protein RelA-associated inhibitor (RAI), containing ankyrin repeats and interacting with the central region of p65 that blocks the DNA binding activity of NF-κB [25,26], similar to the cytoplasmic inhibitors IκBs.

There is accumulating evidence indicating that RNA helicase A (RHA) acts as a transcriptional coactivator. RHA was found to interact with the CREB-binding protein (CBP) [27] and BRCA1 [28], and to be required for transcriptional activation. The ATP binding and/or ATP hydrolysis activities of RHA appear to be required for transcriptional activation as the RHA mutant, in which Lys417 within the conserved ATP-binding motif is substituted by Arg, resulted in the loss of RHA activity and a great reduction in transcriptional activity [27].

In this study, we demonstrate that RHA interacts directly with p65 and activates NF-κB-mediated transcription. We confirmed the interaction between p65 and RHA *in vitro* using the bacterially expressed fusion proteins and an *in vivo* co-immunoprecipitation assay. Depletion of endogenous RHA using siRNA reduced the NF-κB-mediated gene expression. These data indicate that RHA mediates the transcriptional activity of NF-κB.

Experimental procedures

Plasmids

Mammalian expression vector plasmids Gal4-Sp1, pCMV-NIK, ICAM-1-luc (−339 to −30) and E-selectin-luc, IFN-β-luc were generous gifts from S. T. Smale (UCLA School of Medicine, Los Angeles, CA, USA), D. Wallach (Weitzmann Institute of Science, Rehovot, Israel), L. A. Madge and J. S. Pober (Yale University School of Medicine, New Haven, CT, USA), and T. Taniguchi (Tokyo University, Tokyo, Japan), respectively. pCMV-RHA, pCMV-RHA-mATP, pCMV-p65, pGal4-p65, pGBT-p65(1–286), pGBT-p65(286–442), and pGBT-p65(473–522) had been described previously [23,29]. To create pACT2-RHA, the RHA cDNA was amplified by PCR using pCMV-RHA as a template with oligonucleotides containing *Bam*HI-*Xho*I site. These products were digested with *Bam*HI-*Xho*I, and subcloned in-frame into pACT2 vector at the *Bam*HI-*Sal*I site. Construction of a luciferase reporter plasmid, 4κB-luc, containing four tandem copies of the HIV-κB sequence upstream of minimal simian virus 40 (SV40) promoter had been described previously [30]. The other luciferase reporter plasmid, pGal4-luc (pFR-luc), containing five tandem copies of Gal4 binding site upstream of the TATA box, was purchased from Stratagene.

Yeast two-hybrid screening and protein–protein interaction assay

The yeast two-hybrid screening was performed as described previously [23,24,26]. The C-terminal regions of p65 corresponding to amino acids 286–442/477–521 was fused in-frame to Gal4 DNA binding domain (positions 1–147) using the pGBT9 vector (Clontech), and used as a bait for library screening. Yeast strain Y190 was transformed with pGBT-p65-(286–442/477–521) and the human placenta cDNA expression library fused to the Gal4 transactivation domain in the pACT2 vector (Clontech). Approximately one million transformants were screened for their ability to grow on the plates with medium lacking Trp, Leu, and His, and containing 25 mM 3-aminotriazole. Plasmids were rescued from clones that were positive for β-galactosidase activity and identified by nucleotide sequencing. cDNA sequences and their amino acid sequences were compared with GenBank™ and Swiss-Prot databases for identification of the interacting proteins.

Cell culture and transfection

Human embryonic kidney (HEK 293) cells were maintained in DMEM with 10% fetal bovine serum, 100 $U \cdot mL^{-1}$ of penicillin and 100 $\mu g \cdot mL^{-1}$ of streptomycin. Cells were transfected using Fugene-6 transfection reagent (Roche Molecular Biochemicals) according to the manufacturer's

instruction. At 48 h post-transfection, the cells were harvested, and the extracts were prepared for luciferase assay. Luciferase activity was measured by the Luciferase Assay System (Promega, Madison, WI) as described previously [26]. Transfection efficiency was monitored by *Renilla* luciferase activity using the pRL-TK plasmid (Promega) as an internal control. The data are presented as the fold increase in luciferase activities (mean ± SD) relative to the control of three independent transfections. Human recombinant TNF-α was purchased from Roche.

In vitro binding assay

Glutathione-*S* transferase (GST)-RHA(1–250), GST-RHA (244–649), GST-RHA(646–1016), and GST-RHA(1014–1279) were prepared as described previously [29]. These GST-RHA fusion proteins were expressed in *Escherichia coli* strain DH5α and purified. The *in vitro* protein–protein interaction assay ('pull-down' assay) was carried out as described previously [23,24,26]. The p65 protein was synthesized and labeled with [^{35}S]methionine by *in vitro* transcription/translation procedure using a TNT wheat germ extract coupled system (Promega) according to the manufacturer's protocol. Approximately 20 μg of GST fusion proteins was immobilized on 20 μL of glutathione-Sepharose beads and washed 2× with 1 mL of modified HEMNK buffer [20 mM HEPES/KOH (pH 7.5), 100 mM KCl, 12.5 mM $MgCl_2$, 0.2 mM EDTA, 0.3% NP-40, 1 mM dithiothreitol, 0.5 mM phenylmethylsulfonyl fluoride). The beads were left in 0.6 mL of HEMNK and were incubated with radiolabeled proteins for 2 h at 4 °C with gentle mixing. The beads were then washed 3× with 1 mL of HEMNK buffer and 2× with 1 mL of HEMNK buffer containing 150 mM KCl. Bound radiolabeled proteins were eluted with 30 μL of Laemmli sample buffer, boiled for 3 min, and resolved by 10% SDS/PAGE.

Co-immunoprecipitation and Western blot assays

HEK 293 cells were transfected with pCMV-p65 in combination with either CMV-Flag-RHA or the empty vector. After transfection, cells were cultured for 48 h and harvested with lysis buffer [25 mM HEPES/NaOH (pH 7.9), 150 mM NaCl, 1.5 mM $MgCl_2$, 0.2 mM EDTA, 0.3% NP-40, 5% glycerol, 1 mM dithiothreitol, 0.5 mM phenylmethylsulfonyl fluoride]. The lysates were incubated with 10 μL of anti-Flag M2 Affinity Gel (Sigma) at 4 °C for 1 h. The beads were washed 5× with 1 mL of lysis buffer. Antibody-bound complexes were eluted by boiling in Laemmli sample buffer, resolved by 10% SDS/PAGE, and transferred on nitrocellulose membrane (Hybond-C, Amersham). The membrane was incubated with anti-Flag Ig (Sigma) or anti-p65 Ig (Santa Cruz) and the immunoreactive proteins were visualized by enhanced chemiluminescence (SuperSignal, Pierce) as described previously [23,24,26]. To evaluate the level of exogenous p65 expressed from pCMV-p65 containing the His epitope-tag, rabbit polyclonal anti-$(His)_6$ Ig (Santa Cruz) was used for Western blotting.

RNA interference

The double-stranded RNA specific for RHA was synthesized by Takara Bio Inc. (Shiga, Japan). This RHA specific small interference RNA (siRNA) 5′-GCAUAAAACUUCUGC GUCU-3′ was targeted to the RHA portion from 2408 to 2426. Control siRNA 5′-AUUCUAUCACUAGCGU GAC-3′ was purchased from Dharmacon (Lafayette, CO, USA). siRNA transfections were performed using lipofectamine 2000 reagent (Invitrogen) according to the manufacturer's instruction.

Results

Identification of RHA as a p65-binding protein

To identify proteins interacting with p65 subunit of NF-κB, we performed the yeast two-hybrid screen using pGBT-p65(286–442/477–521) as a bait for the screening. Yeast strain Y 190 was used for the screening of a human placenta cDNA library fused to the Gal4 transcriptional activation domain in the pACT2 vector (Clontech). Among $\approx 1.0 \times 10^6$ Y190 yeast transformants, 90 colonies grew on selective medium and turned blue when tested with a β-galactosidase assay. Each plasmid purified from the positive colony was cotransfected with the bait plasmid into the yeast to confirm the specific interaction. DNA sequencing and comparison with GenBank and SwissProt databases revealed the gene for RHA (one clone) in addition to IκBα/MAD3 (five clones) and Bcl3 (one clone) that are known to interact with p65.

In order to map the interaction domain of p65 with RHA, we performed the yeast two-hybrid protein–protein interaction assay (Table 1, Fig. 1B). Various regions of the p65 protein were fused to Gal4-DNA binding domain in the pGBT9 vector and cotransfected with pACT2-RHA, encoding RHA fused to Gal4–transactivation domain. Interactions were tested by β-galactosidase activity (Table 1) and by growth of yeast cells on plates with medium lacking His, Leu and Trp, and containing 25 mM 3-aminotriazole (Fig. 1B). pGBT-p65(1–286), pGBT-p65(286–442), and

Table 1. Yeast two-hybrid interaction assays between p65 and RHA. Yeast Y190 cells were cotransformed with expression vectors encoding various proteins fused to Gal4 DNA-binding domain (Gal4-DBD) and Gal4 transcriptional activation domain (Gal4-AD). pACT2-RHA is a rescued clone which encodes full length RHA fused to Gal4-AD. pACT2-IκBα encodes full length IκBα (amino acids 1–317) fused to Gal4-AD. Leu^+ Trp^+ transformants were streaked on selective medium lacking Leu and Trp, and allowed to grow for 2 days at 30 °C. At least three colonies of each transformant were tested for β-galactosidase activity using X-gal colony filter assay (Clontech). +, positive for β-galactosidase activity (blue colony) after 2–3 h; –, no β-galactosidase activity (white colony) after 24 h; ND, not determined.

	Gal4-AD hybrid		
Gal4-DBD hybrid	pACT2	pACT2-RHA	pACT2-IκBα
pGBT9	–	–	–
pGBT-p65(1–286)	–	–	–
pGBT-p65(286–551)	+	ND	ND
pGBT-p65(286–521)	+	ND	ND
pGBT-p65(286–470)	+	ND	ND
pGBT-p65(286–442)	–	–	+
pGBT-p65(473–522)	–	+	–

pGBT-p65(473–522) alone did not show any background in the prototrophic selection or in the β-galactosidase assay. Among these, pGBT-p65(473–522) was shown to interact with pACT2-RHA (Table 1, Fig. 1B). These results indicate that the minimal region of p65 responsible for the interaction with RHA resides within the amino acids 473–522.

Binding of RHA to p65

To confirm the interaction between RHA and p65, we performed an *in vitro* protein–protein interaction assay using various recombinant RHA proteins in fusion with GST. The radiolabeled p65 protein was synthesized by *in vitro* transcription/translation in the presence of [^{35}S]methionine using wheat germ extract. The radiolabeled p65 was incubated with GST-RHA fusion proteins immobilized on glutathione-Sepharose beads. As shown in Fig. 1C, p65 bound to GST-RHA(1–250) and GST-RHA(244–649) but not to GST-RHA(646–1016), or GST-RHA(1014–1279). No p65 binding was detected with beads containing GST alone (as a negative control).

To investigate the interaction between RHA and p65 *in vivo*, we expressed p65 and RHA containing the Flag-epitope in the N-terminus in HEK 293 cells. Lysates were prepared from the transfected HEK 293 cells and immunoprecipitated with anti-Flag M2 Affinity Gel (Sigma) and the resulting precipitate was disrupted and immunoblotted with anti-p65 and anti-Flag Igs. As shown in Fig. 1D, p65 was co-immunoprecipitated with Flag-RHA. To confirm this interaction, the cell lysates were immunoprecipitated with anti-p65 Ig or control IgG, followed by Western blotting using anti-Flag Ig. As shown in Fig. 1E, Flag-RHA was co-immunoprecipitated with p65. These data indicate the interaction between p65 and RHA *in vivo*.

RHA mediates NF-κB-dependent gene expression

We then investigated the effect of RHA on NF-κB-dependent gene expression. In Fig. 2A, the effect of RHA was examined on gene expression from the reporter plasmid 4κB-luc by transfection of pCMV-p65 with or without cotransfection of pCMV-RHA in HEK 293 cells. RHA augmented the NF-κB-mediated transactivation in a dose-dependent manner when the p65-expression plasmid was cotransfected. pCMV-p65 alone activated gene expression from 4κB-luc, but RHA further enhanced the p65-mediated gene expression. However, there was no detectable effect of RHA on the basal transcription level in the absence of pCMV-p65. These effects of RHA was not through increasing the level of p65, as Western blot analysis of the transfected cell lysate revealed no increase in the protein level of exogenously expressed p65 (Fig. 2A, lower panel). Similarly, RHA augmented NF-κB dependent gene expression induced by TNF-α or by NF-κB inducing kinase (NIK), the upstream kinase for NF-κB activation (Fig. 2B,C).

The catalytic activity is required for the effect of RHA

To determine whether endogenous RHA is involved in NF-κB mediated transcription, we used pCMV-RHAmATP,

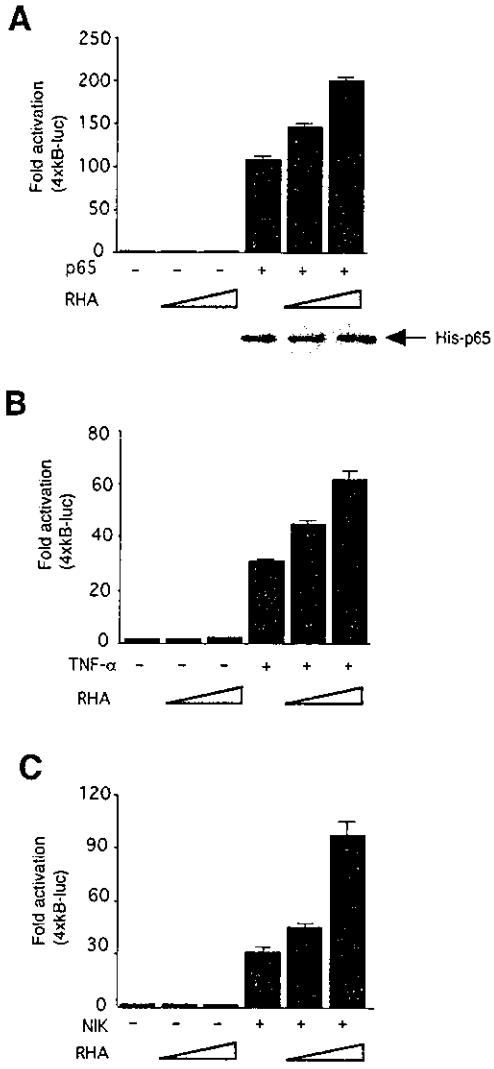

Fig. 2. RHA augments NF-κB-dependent gene expression. (A) HEK 293 cells were transfected with 20 ng of 4κB-luc in combination with pCMV-p65 [containing $(His)_6$ epitope] (10 ng) and pCMV-RHA expression plasmids (50 or 100 ng). Cells were harvested 24 h after transfection, and luciferase activity was measured. Western blot analysis of p65 levels in transfected cell extracts was done to confirm if equal amounts of the exogenous p65 are expressed irrespective of RHA overexpression (lower panel). A portion of each cell extract was separated by 10% SDS/PAGE and immunoblotted with anti-His Ig. (B) Effect of RHA on the NF-κB-dependent gene expression induced by TNF. HEK 293 cells were transfected with 4κB-luc (50 ng) and pCMV-RHA (50 or 100 ng). After 24 h of transfection, cells were stimulated with 1 ng·mL^{-1} of TNF and harvested after additional incubation for 24 h. (C) Effect of RHA on the NF-κB-dependent gene expression induced by NIK. HEK 293 cells were transfected with 4κBw-luc (50 ng) in the absence or presence of pCMV-NIK (10 ng) and pCMV-RHA (50 or 100 ng). Cells were harvested 24 h after transfection, and luciferase activity was measured. Extents of fold activation of luciferase gene expression as compared to the transfection with reporter plasmid alone are indicated. Values (fold activation) represent the mean ± SD of three independent transfections. Similar results were achieved repeatedly.

the expression plasmid for dominant negative mutant RHA, in which Lys417 of the conserved ATP-binding motif (Gly-Lys-Thr) of RHA catalytic domain was substituted by Arg, and the ATPase activity was abolished. NF-κB-dependent gene expression induced by p65, TNF-α and NIK was inhibited by the expression of RHAmATP (Fig. 3A–C), suggesting that the endogenous RHA mediates the transcriptional activity of NF-κB p65.

Effect of RHA on the p65-mediated transactivation of ICAM-1, E-selectin, and IFN-β promoters

To confirm the effect of RHA on NF-κB in physiological promoters, we examined the effect of RHA on the promoters of ICAM-1, E-selectin, and IFN-β containing NF-κB binding sites. Various amounts of RHA expressing plasmid (pCMV-RHA) or RHAmATP plasmid (pCMV-RHAmATP) were transfected into HEK 293 cells along with ICAM-1-luc, E-selectin-luc or IFN-β-luc. As shown in Fig. 4, RHA enhanced the NF-κB dependent transcription for ICAM-1, E-selectin and IFN-β promoters (Fig. 4A–C, left panels). On the other hand, overexpression of RHAmATP inhibited the NF-κB dependent transcription from ICAM-1, E-selectin and IFN-β promoters (Fig. 4A–C, right panels). These data suggest that the enzymatic activity of RHA is involved in the NF-κB mediated gene expression in physiological promoters such as IFN-β, ICAM-1 and E-selectin.

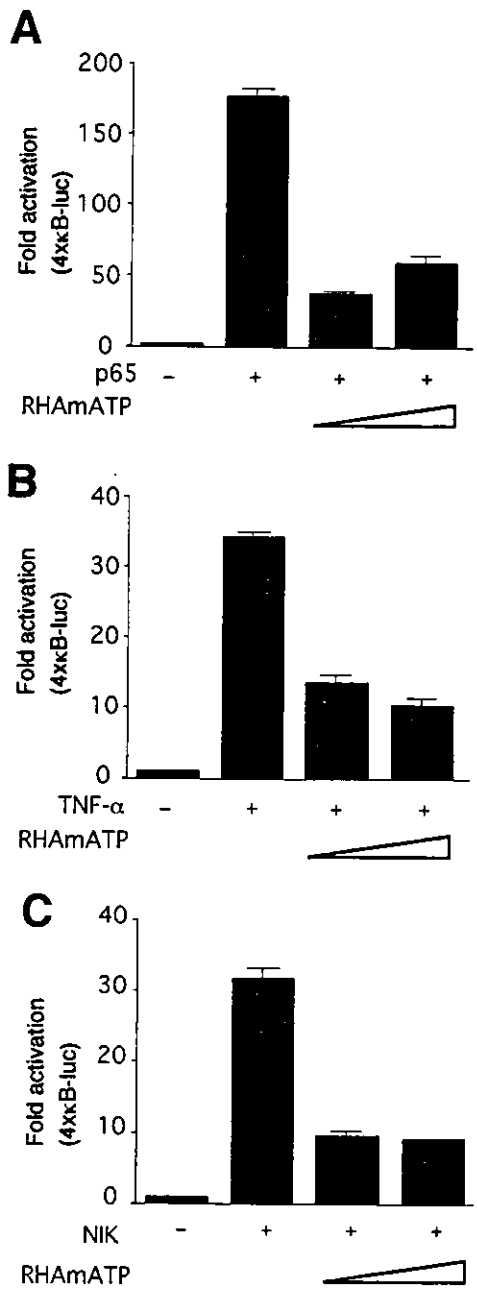

RHA activates NF-κB through activation domain of p65

To further analyze the effect of RHA on p65, we used expression plasmids for fusion proteins of Gal4-p65, Gal4-CREB or Gal4-Sp1 in which the DNA-binding domain of Gal4 was fused with p65, CREB and Sp1. The extents of augmentation of transactivation of these Gal4-p65, Gal4-CREB and Gal4-Sp1 by RHA are shown in Fig. 5. RHA augmented the transactivation mediated by Gal4-p65(1–551) and Gal4-CREB, by 1.9-fold and 3.6-fold, respectively, whereas there was no significant effect on Gal4-Sp1 (Fig. 5A). The effect of RHA on the CREB-mediated transactivation was reported previously [27]. These observations indicated that the effects of RHA on transactivation appeared relatively specific for NF-κB and CREB. To further examine whether the effect of RHA depends on the transactivation domain of p65, we used plasmids expressing various portions of p65 in fusion with Gal4 DNA-binding domain including Gal4-p65(1–551), Gal4-p65(1–286) and Gal4-p65(286–551). As shown in Fig. 5B, RHA augmented the transactivation mediated by Gal4-p65(1–551) and Gal4-p65(286–551) whereas there was no significant effect

Fig. 3. RHAmATP inhibits NF-κB-mediated transcription. (A) Inhibition of p65-mediated transcription by RHA mutant (RHAmATP) containing a single amino acid substitution in the helicase domain that abolishes its ATP-binding and helicase activity. HEK 293 cells were transfected with 20 ng of 4κB-luc in combination with pCMV-p65 (10 ng) or pCMV-RHAmATP expression plasmids (50 or 100 ng). Cells were harvested 24 h after transfection, and the luciferase activity was measured. (B) RHAmATP inhibits NF-κB-dependent transcription induced by TNF-α. HEK 293 cells were transfected with 4κB-luc (50 ng) in combination with pCMV-RHAmATP (50 or 100 ng) or the empty vector. After 24 h of transfection, cells were stimulated with 1 ng·mL^{-1} of TNF and harvested after additional incubation for 24 h (C) RHAmATP inhibits NF-κB-dependent transcription induced by NIK. HEK 293 cells were transfected with 4κBw-luc (50 ng) in combination with pCMV-NIK (10 ng) and pCMV-RHAmATP (50 or 100 ng). Cells were harvested 24 h after transfection, and the luciferase activity was measured. pCMV control plasmids were included such that all transfections had equivalent amounts of expression plasmid. Total DNA was kept at 0.5 μg with pUC19 plasmid. Cells were harvested 48 h after transfection, and luciferase activity was measured. Extents of fold activation of luciferase gene expression as compared to the transfection with reporter plasmid alone are indicated. Values (fold activation) represent the mean ± SD of three independent transfections. Similar results were achieved repeatedly.

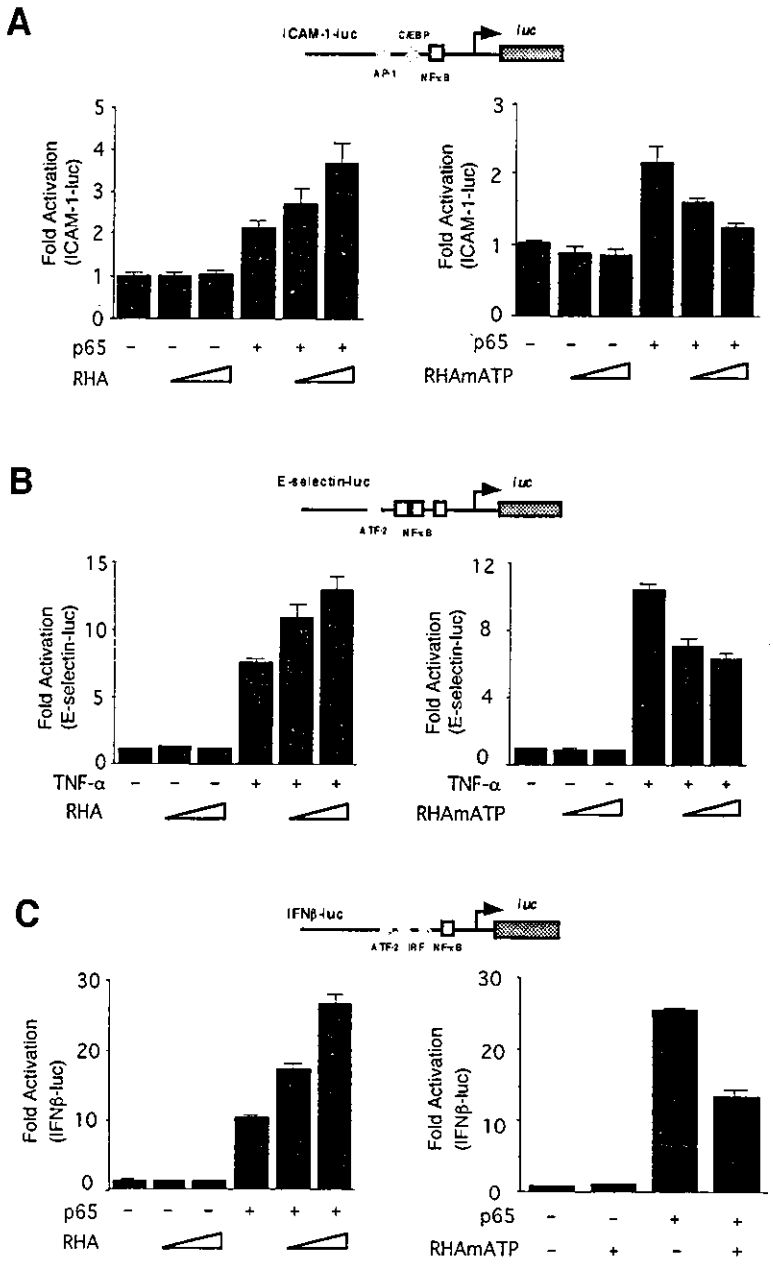

Fig. 4. RHA mediates NF-κB-dependent transcription in physiological promoters. (A) Effect of RHA on ICAM-1 promoter activity. HEK 293 cells were transfected with ICAM-1-luc (20 ng) in combination with pCMV-p65 (10 ng) and pCMV-RHA (50 or 100 ng) or pCMV-RHAmATP (50 or 100 ng). After 24 h of transfection, cells were harvested and luciferase activity was measured. (B) Effect of RHA on E-selectin promoter activity. HEK 293 cells were transfected with 20 ng of E-selectin-luc in combination with pCMV-RHA (50 or 100 ng) or pCMV-RHAmATP (50 or 100 ng). After 24 h of transfection, cells were stimulated with 1 ng·mL^{-1} of TNF-α and harvested after additional incubation for 24 h. (C) Effects of RHA on IFN-β promoter activity. HEK 293 cells were transfected with 20 ng of IFN-β-luc in combination with pCMV-p65 (10 ng) and pCMV-RHA (50 or 100 ng) or pCMV-RHAmATP (100 ng). After 24 h of transfection, cells were harvested and luciferase activity was measured. Values (fold activation) represent the mean ± SD of three independent transfections.

on Gal4-p65(1–286). These observations indicated that the C-terminal domain of p65 is required for the action of RHA.

Effect of RHA knockdown on the NF-κB-mediated transactivation

Finally, we investigated the physiological role of endogenous RHA with the use of RNA interference. We synthesized RNA duplex directed against the RHA-coding sequence (the nucleotide portion from 2408 to 2426). Transfection of HEK 293 cells with the RHA specific siRNA reduced the endogenous RHA protein level. The control siRNA had no effect (Fig. 6A). Neither RHA siRNA nor control siRNA had any effect on p65 and α-tubulin protein levels. We then examined the effect of RHA depletion on the NF-κB dependent reporter gene expression. As shown in Fig. 6B, the RHA siRNA reduced the NF-κB dependent gene expression from 4κB-luc induced by TNF-α. Similarly, we examined the effect of RHA siRNA on the TNF-mediated activation of E-selectin promoter. As shown in Fig. 6C, RHA siRNA significantly reduced the TNF-mediated induction of E-selectin gene expression. These data indicate that endogenous RHA is involved in the NF-κB-mediated gene expression.

Discussion

In this study we found that the NF-κB p65 subunit interacts with RHA *in vitro* and *in vivo*. Transient transfection assays revealed that RHA is positively involved in the

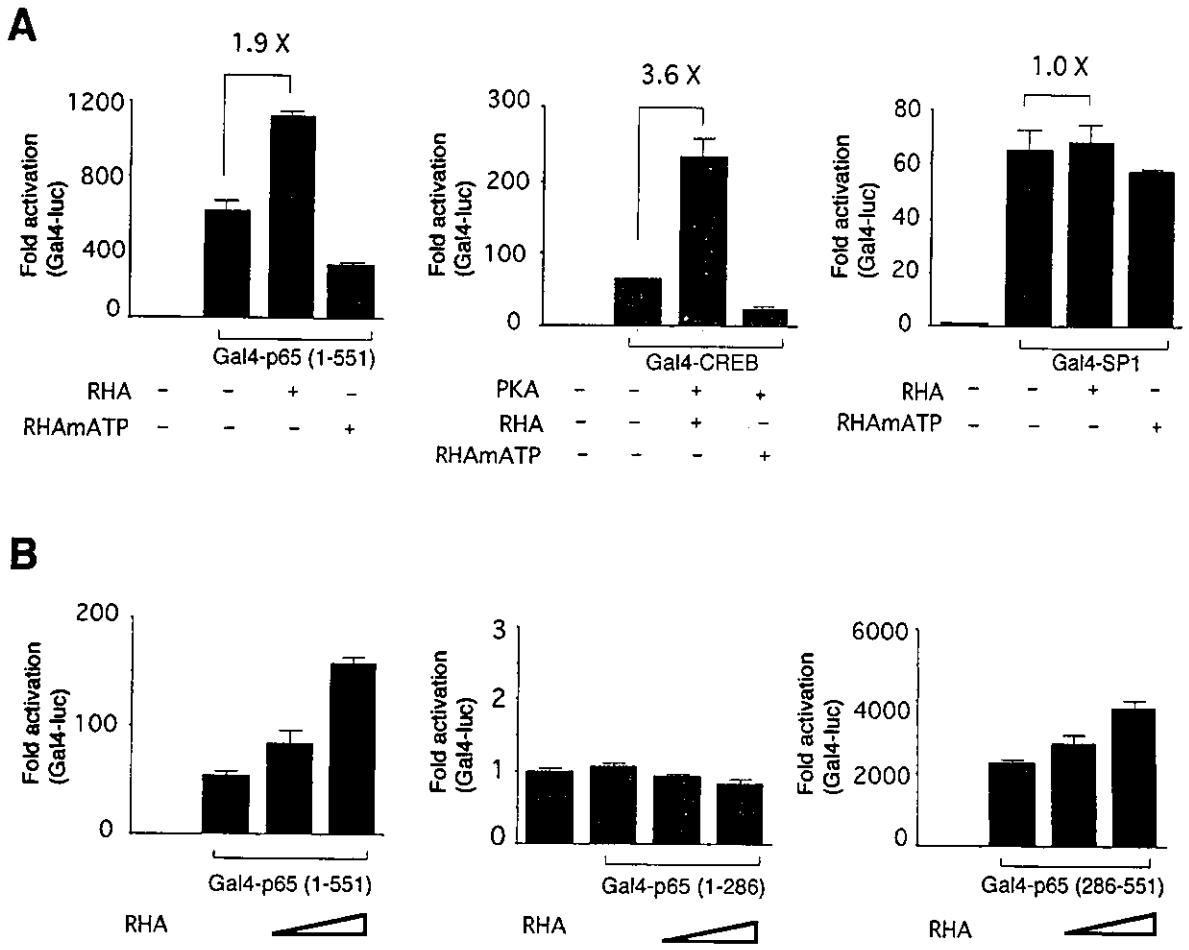

Fig. 5. Effects of RHA on Gal4-p65, Gal4-CREB and Gal4-Sp1-mediated transcription. (A) HEK 293 cells were transfected with 50 ng of 5x Gal4-luc reporter plasmid together with 10 ng of Gal4-p65 (left panel) or Gal4-CREB (10 ng) and PKA (10 ng) (middle panel) or Gal4-Sp1 (100 ng) (right panel) in combination with pCMV-RHA (100 ng) or pCMV-RHAmATP (100 ng). Cells were harvested 24 h after transfection and the luciferase activity was measured. Extents of fold activation of luciferase gene expression as compared to the transfection with reporter plasmid alone are indicated. (B) HEK 293 cells were transfected with 5x Gal4-luc reporter plasmid (50 ng) together with 10 ng of each of Gal4-p65 (1–551) (left panel), Gal4-p65 (1–286) (middle panel), Gal4-p65 (286–551) (right panel) and pCMV-RHA (100 or 200 ng). Cells were harvested 24 h after transfection, and luciferase activity was measured. Extents of fold activation of luciferase gene expression as compared to the transfection with reporter plasmid alone are indicated. Values (fold activation) represent the mean ± SD of three independent transfections.

NF-κB-dependent gene expression such as E-selectin, ICAM-1 and IFN-β. As NF-κB-dependent gene expression was inhibited by the dominant negative mutant form of RHA (RHAmATP) lacking the ATP-binding and helicase activity, the enzymatic activity of RHA is required for the transcriptional activation mediated by NF-κB.

RHA is a nucleic acid helicase that unwinds double-stranded DNA and RNA in ATP-dependent manner. It belongs to a large family of RNA helicases containing DEXD/H box that are known to be involved in various steps of gene expression including transcription, editing, splicing, RNA export, translation, and RNA turnover [31]. It is considered that RNA helicases prompt RNA molecules to initiate the interaction with other RNA molecules or proteins by catalyzing the folding and unfolding of these RNA molecules, just as proteins require chaperones to assist in folding and unfolding to form appropriate conformation [32,33].

RHA consists of two double-stranded RNA binding domains at the N-terminus, a helicase catalytic domain in the central part, and a Gly-rich single-stranded nucleic acid binding domain (RGG-box) at the C-terminus. Sequence analysis revealed that RHA contains seven helicase core motifs DEXD/H that are conserved among the helicase superfamily. It was shown previously that RHA stimulates transcription by interacting with CBP, BRCA1, and RNA Pol II [27,28]. Members of the ATPase/helicase family play important roles in many transcriptional processes including initiation, elongation, termination, and nuclear export [31]. For example, ATPase/helicase activity is found associated with TFIIH and chromatin remodeling complexes and plays crucial roles in transcriptional initiation and preinitiation. The ATPase/helicase activity of XPB/ERCC3 contained in TFIIH is required for promoter opening [34,35]. Similarly, the ATPase/helicase activity of SWI2/SNF2 in the chromatin remodeling complex SWI/SNF is involved

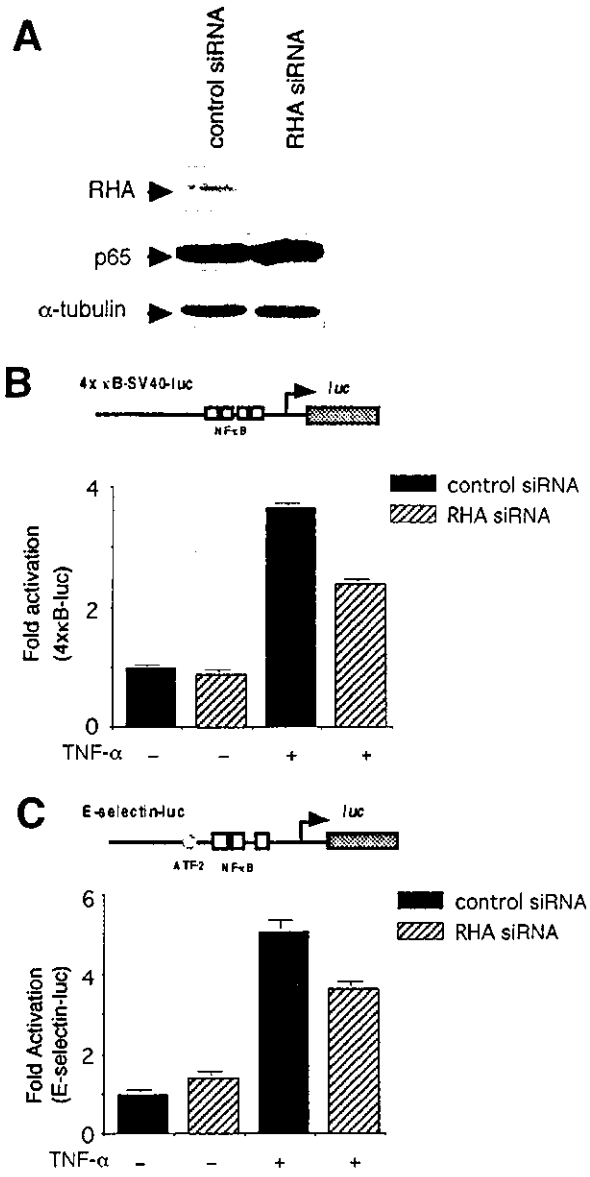

Fig. 6. Effect of RHA knockdown on NF-κB-mediated transactivation. (A) Knockdown of RHA by siRNA. HEK 293 cells (5×10^5) were transfected with 200 pmol of siRNA targeted to RHA. For the siRNA control, double-stranded RNA of unrelated sequences was used. The siRNA was transfected with lipofectamine 2000. After 48 h of transfection, cells were lysed and immunoblotted with antibodies to RHA, p65 and α-tubulin. (B) Inhibition of TNF-mediated NF-κB activation by RHA siRNA. HEK 293 cells (10^5) were transfected with 20 pmol of RHA siRNA or control siRNA together with 4κB-luc (20 ng). After 24 h of transfection, cells were stimulated with 10 ng·mL^{-1} of TNF-α and harvested after additional incubation for 24 h. (C) Inhibition of TNF-mediated E-selectin gene expression by RHA siRNA. HEK 293 cells (10^5) were transfected with 20 pmol of RHA siRNA or control siRNA together with E-selectin-luc (20 ng). After 24 h of transfection, cells were stimulated with 10 ng·mL^{-1} of TNF-α and harvested after additional incubation for 24 h. Extents of fold activation of luciferase gene expression as compared to the transfection with reporter plasmid alone are indicated. Values (fold activation) represent the means ± SD of three independent transfections. Similar results were obtained repeatedly.

in the relaxation of chromatin structure and promotes efficient transcription [36].

RHA was originally isolated as a human homologue of *Drosophila* maleless protein (MLE) [37]. MLE is involved in sex-specific gene dosage compensation and elevates the level of transcription derived from a single X-chromosome in male flies to a level equivalent to that derived from two X chromosomes in female flies [38]. MLE increases the transcriptional activity of X-linked genes through interaction with male-specific lethal (MSL) complexes [39,40]. In addition, the ATPase activity of RHA and that of MLE appeared to be essential for the CREB-dependent gene expression in mammals [27] and the gene dosage compensation in *Drosophila* [41], respectively. As MLE and its interaction with MSL are required for the specific histone H4 acetylation on X-chromosome [42,43], MLE may activate transcription of X-chromosome genes by promoting chromatin remodeling.

Another RNA helicase, p68 helicase belonging to the DEAD-box protein family, was shown to interact with human estrogen receptor α (ERα) and to act as a coactivator for ERα [44]. Although it was reported that RHA enhanced the CREB-dependent gene expression by bridging CBP and RNA Pol II, there has been no direct evidence that RHA interacts with CREB or any other gene-specific transactivators. In this study, we found that RHA binds to p65 through the interaction between the N-terminal region of RHA and the C-terminal GIR of p65. As the TA1-like and TA1 domains of p65 themselves recruit CBP/p300 coactivators, RHA appears to further facilitate the coactivator recruitment or assembly of transactivation complex by interaction with RNA Pol II.

Interestingly, we have reported previously that FUS/TLS activates the NF-κB-mediated transcription by interacting with the same region of p65 (amino acids 473–522) (GIR) [24]. There are some similarities between RHA and FUS/TLS. First, these proteins contain RGG domain that is capable of binding single-strand nucleic acids [45,46]. Second, they interact directly with the largest subunit of RNA Pol II and coactivator CBP/p300 [27,47]. Thus, NF-κB appears to form a functional transactivation complex ('enhanceosome') containing RHA, FUS/TLS, CBP/p300, RNA Pol II, and general transcription factors. Further studies are needed to clarify the action of RHA in transcriptional regulation.

Acknowledgements

We thank Drs S. T. Smale, D. Wallach, L. A. Madge, J. S. Pober, T. Nakajima, and T. Taniguchi for their generosity in providing the plasmids and RHA-antibody and Ms Angelita Sarile for language edition. We also thank Dr K. Imai and other laboratory members for critical discussions. This work was supported in part by grants-in-aid from the Ministry of Health, Labor and Welfare, the Ministry of Education, Culture, Sports, Science, and Technology of Japan and the Japanese Health Sciences Foundation.

References

1. Baldwin, A.S. Jr (1996) The NF-kappa B and I kappa B proteins: new discoveries and insights. *Annu. Rev. Immunol.* **14**, 649–683.

2. Ghosh, S. & Karin, M. (2002) Missing pieces in the NF-kappaB puzzle. *Cell* **109**, S81–S96.
3. Silverman, N. & Maniatis, T. (2001) NF-kappaB signaling pathways in mammalian and insect innate immunity. *Genes Dev.* **15**, 2321–2342.
4. Karin, M. & Lin, A. (2002) NF-kappaB at the crossroads of life and death. *Nat. Immunol.* **3**, 221–227.
5. Tak, P.P. & Firestein, G.S. (2001) NF-kappaB: a key role in inflammatory diseases. *J. Clin. Invest.* **107**, 7–11.
6. Yoza, B.K., Hu, J.Y. & McCall, C.E. (1996) Protein-tyrosine kinase activation is required for lipopolysaccharide induction of interleukin 1beta and NFkappaB activation, but not NFkappaB nuclear translocation. *J. Biol. Chem.* **271**, 18306–18309.
7. Bergmann, M., Hart, L., Lindsay, M., Barnes, P.J. & Newton, R. (1998) IkappaBalpha degradation and nuclear factor-kappaB DNA binding are insufficient for interleukin-1beta and tumor necrosis factor-alpha-induced kappaB-dependent transcription. Requirement for an additional activation pathway. *J. Biol. Chem.* **273**, 6607–6610.
8. Schmitz, M.L., Stelzer, G., Altmann, H., Meisterernst, M. & Baeuerle, P.A. (1995) Interaction of the COOH-terminal transactivation domain of p65 NF-kappa B with TATA-binding protein, transcription factor IIB, and coactivators. *J. Biol Chem.* **270**, 7219–7226.
9. Perkins, N.D., Felzien, L.K., Betts, J.C., Leung, K., Beach, D.H. & Nabel, G.J. (1997) Regulation of NF-kappaB by cyclin-dependent kinases associated with the p300 coactivator. *Science* **275**, 523–527.
10. Gerritsen, M.E., Williams, A.J., Neish, A.S., Moore, S., Shi, Y. & Collins, T. (1997) CREB-binding protein/p300 are transcriptional coactivators of p65. *Proc. Natl Acad. Sci. USA* **94**, 2927–2932.
11. Schmitz, M.L., dos Santos Silva, M.A. & Baeuerle, P.A. (1995) Transactivation domain 2 (TA2) of p65 NF-kappa B. Similarity to TA1 and phorbol ester-stimulated activity and phosphorylation in intact cells. *J. Biol. Chem.* **270**, 15576–15584.
12. Jiang, X., Takahashi, N., Matsui, N., Tetsuka, T. & Okamoto, T. (2003) The NF-kappa B activation in lymphotoxin beta receptor signaling depends on the phosphorylation of p65 at serine 536. *J. Biol. Chem.* **278**, 919–926.
13. Sakurai, H., Chiba, H., Miyoshi, H., Sugita, T. & Toriumi, W. (1999) IkappaB kinases phosphorylate NF-kappaB p65 subunit on serine 536 in the transactivation domain. *J. Biol. Chem.* **274**, 30353–30356.
14. Sakurai, H., Suzuki, S., Kawasaki, N., Nakano, H., Okazaki, T., Chino, A., Doi, T. & Saiki, I. (2003) Tumor necrosis factor-alpha-induced IKK phosphorylation of NF-kappaB p65 on serine 536 is mediated through the TRAF2, TRAF5, and TAK1 signaling pathway. *J. Biol. Chem.* **278**, 36916–36923.
15. Zhong, H., SuYang, H., Erdjument-Bromage, H., Tempst, P. & Ghosh, S. (1997) The transcriptional activity of NF-kappaB is regulated by the IkappaB-associated PKAc subunit through a cyclic AMP-independent mechanism. *Cell* **89**, 413–424.
16. Zhong, H., May, M.J., Jimi, E. & Ghosh, S. (2002) The phosphorylation status of nuclear NF-kappa B determines its association with CBP/p300 or HDAC-1. *Mol. Cell* **9**, 625–636.
17. Sheppard, K.A., Rose, D.W., Haque, Z.K., Kurokawa, R., McInerney, E., Westin, S., Thanos, D., Rosenfeld, M.G., Glass, C.K. & Collins, T. (1999) Transcriptional activation by NF-kappaB requires multiple coactivators. *Mol. Cell. Biol.* **19**, 6367–6378.
18. Naar, A.M., Beaurang, P.A., Zhou, S., Abraham, S., Solomon, W. & Tjian, R. (1999) Composite co-activator ARC mediates chromatin-directed transcriptional activation. *Nature* **398**, 828–832.
19. Xu, X., Prorock, C., Ishikawa, H., Maldonado, E., Ito, Y. & Gelinas, C. (1993) Functional interaction of the v-Rel and c-Rel oncoproteins with the TATA-binding protein and association with transcription factor IIB. *Mol. Cell. Biol.* **13**, 6733–6741.
20. Blair, W.S., Bogerd, H.P., Madore, S.J. & Cullen, B.R. (1994) Mutational analysis of the transcription activation domain of RelA: identification of a highly synergistic minimal acidic activation module. *Mol. Cell. Biol.* **14**, 7226–7234.
21. Kerr, L.D., Ransone, L.J., Wamsley, P., Schmitt, M.J., Boyer, T.G., Zhou, Q., Berk, A.J. & Verma, I.M. (1993) Association between proto-oncoprotein Rel and TATA-binding protein mediates transcriptional activation by NF-kappa B. *Nature* **365**, 412–419.
22. Yamit-Hezi, A., Nir, S., Wolstein, O. & Dikstein, R. (2000) Interaction of TAFII105 with selected p65/RelA dimers is associated with activation of subset of NF-kappa B genes. *J. Biol. Chem.* **275**, 18180–18187.
23. Tetsuka, T., Uranishi, H., Imai, H., Ono, T., Sonta, S., Takahashi, N., Asamitsu, K. & Okamoto, T. (2000) Inhibition of nuclear factor-kappaB–mediated transcription by association with the amino-terminal enhancer of split, a Groucho-related protein lacking WD40 repeats. *J. Biol. Chem.* **275**, 4383–4390.
24. Uranishi, H., Tetsuka, T., Yamashita, M., Asamitsu, K., Shimizu, M., Itoh, M. & Okamoto, T. (2001) Involvement of the pro-oncoprotein TLS (translocated in liposarcoma) in nuclear factor-kappa B p65-mediated transcription as a coactivator. *J. Biol. Chem.* **276**, 13395–13401.
25. Takada, N., Sanda, T., Okamoto, H., Yang, J.P., Asamitsu, K., Sarol, L., Kimura, G., Uranishi, H., Tetsuka, T. & Okamoto, T. (2002) RelA-associated inhibitor blocks transcription of human immunodeficiency virus type 1 by inhibiting NF-kappaB and Sp1 actions. *J. Virol.* **76**, 8019–8030.
26. Yang, J.P., Hori, M., Sanda, T. & Okamoto, T. (1999) Identification of a novel inhibitor of nuclear factor-kappaB, RelA-associated inhibitor. *J. Biol. Chem.* **274**, 15662–15670.
27. Nakajima, T., Uchida, C., Anderson, S.F., Lee, C.G., Hurwitz, J., Parvin, J.D. & Montminy, M. (1997) RNA helicase A mediates association of CBP with RNA polymerase II. *Cell* **90**, 1107–1112.
28. Anderson, S.F., Schlegel, B.P., Nakajima, T., Wolpin, E.S. & Parvin, J.D. (1998) BRCA1 protein is linked to the RNA polymerase II holoenzyme complex via RNA helicase A. *Nat. Genet.* **19**, 254–256.
29. Yang, J.P., Tang, H., Reddy, T.R. & Wong-Staal, F. (2001) Mapping the functional domains of HAP95, a protein that binds RNA helicase A and activates the constitutive transport element of type D retroviruses. *J. Biol. Chem.* **276**, 30694–30700.
30. Sato, T., Asamitsu, K., Yang, J.P., Takahashi, N., Tetsuka, T., Yoneyama, A., Kanagawa, A. & Okamoto, T. (1998) Inhibition of human immunodeficiency virus type 1 replication by a bioavailable serine/threonine kinase inhibitor, fasudil hydrochloride. *AIDS Res. Hum. Retroviruses* **14**, 293–298.
31. Tanner, N.K. & Linder, P. (2001) DExD/H box RNA helicases: from generic motors to specific dissociation functions. *Mol. Cell* **8**, 251–262.
32. Tanner, N.K. (1999) Ribozymes: the characteristics and properties of catalytic RNAs. *FEMS Microbiol. Rev.* **23**, 257–275.
33. Richardson, A., Landry, S.J. & Georgopoulos, C. (1998) The ins and outs of a molecular chaperone machine. *Trends Biochem. Sci.* **23**, 138–143.
34. Drapkin, R., Reardon, J.T., Ansari, A., Huang, J.C., Zawel, L., Ahn, K., Sancar, A. & Reinberg, D. (1994) Dual role of TFIIH in DNA excision repair and in transcription by RNA polymerase II. *Nature* **368**, 769–772.
35. Tirode, F., Busso, D., Coin, F. & Egly, J.M. (1999) Reconstitution of the transcription factor TFIIH: assignment of functions for the three enzymatic subunits, XPB, XPD, and cdk7. *Mol. Cell* **3**, 87–95.

36. Schnitzler, G., Sif, S. & Kingston, R.E. (1998) Human SWI/SNF interconverts a nucleosome between its base state and a stable remodeled state. *Cell* **94**, 17–27.
37. Lee, C.G. & Hurwitz, J. (1993) Human RNA helicase A is homologous to the maleless protein of *Drosophila*. *J. Biol. Chem.* **268**, 16822–16830.
38. Kuroda, M.I., Kernan, M.J., Kreber, R., Ganetzky, B. & Baker, B.S. (1991) The maleless protein associates with the X chromosome to regulate dosage compensation in *Drosophila*. *Cell* **66**, 935–947.
39. Meller, V.H., Wu, K.H., Roman, G., Kuroda, M.I. & Davis, R.L. (1997) roX1 RNA paints the X chromosome of male *Drosophila* and is regulated by the dosage compensation system. *Cell* **88**, 445–457.
40. Amrein, H. & Axel, R. (1997) Genes expressed in neurons of adult male *Drosophila*. *Cell* **88**, 459–469.
41. Lee, C.G., Chang, K.A., Kuroda, M.I. & Hurwitz, J. (1997) The NTPase/helicase activities of *Drosophila* maleless, an essential factor in dosage compensation. *EMBO J.* **16**, 2671–2681.
42. Bone, J.R., Lavender, J., Richman, R., Palmer, M.J., Turner, B.M. & Kuroda, M.I. (1994) Acetylated histone H4 on the male X chromosome is associated with dosage compensation in *Drosophila*. *Genes Dev.* **8**, 96–104.
43. Rastelli, L. & Kuroda, M.I. (1998) An analysis of maleless and histone H4 acetylation in *Drosophila melanogaster* spermatogenesis. *Mech. Dev.* **71**, 107–117.
44. Endoh, H., Maruyama, K., Masuhiro, Y., Kobayashi, Y., Goto, M., Tai, H., Yanagisawa, J., Metzger, D., Hashimoto, S. & Kato, S. (1999) Purification and identification of p68 RNA helicase acting as a transcriptional coactivator specific for the activation function 1 of human estrogen receptor alpha. *Mol. Cell. Biol.* **19**, 5363–5372.
45. Zhang, S. & Grosse, F. (1997) Domain structure of human nuclear DNA helicase II (RNA helicase A). *J. Biol. Chem.* **272**, 11487–11494.
46. Burd, C.G. & Dreyfuss, G. (1994) Conserved structures and diversity of functions of RNA-binding proteins. *Science* **265**, 615–621.
47. Yang, L., Embree, L.J. & Hickstein, D.D. (2000) TLS-ERG leukemia fusion protein inhibits RNA splicing mediated by serine-arginine proteins. *Mol. Cell. Biol.* **20**, 3345–3354.

Available online at www.sciencedirect.com
SCIENCE DIRECT®
Biochemical and Biophysical Research Communications 315 (2004) 434–438
BBRC
www.elsevier.com/locate/ybbrc

Expression of 53BP2 and ASPP2 proteins from TP53BP2 gene by alternative splicing

Naoko Takahashi, Shinya Kobayashi, Xu Jiang, Koji Kitagori, Kenichi Imai, Yurina Hibi, and Takashi Okamoto*

Department of Molecular and Cellular Biology, Nagoya City University Graduate School of Medical Sciences, 1 Kawasumi, Mizuho-cho, Mizuho-ku, Nagoya 467-8601, Japan

Received 19 December 2003

Abstract

The p53 binding protein 2 (53BP2) has been initially identified as an interacting protein to p53 and subsequent studies have shown that it also interacts with Bcl-2 and NF-κB p65 subunit. We have previously found that the TP53BP2 gene encoding 53BP2 protein is a single copy gene and has been mapped to the long arm of chromosome 1 at q42.1. The subsequent studies revealed that TP53BP2 encodes two proteins, 53BP2 and ASPP2, of 1005 and 1128 amino acids, respectively. ASPP2 contains additional 123 amino acids to the N-terminus of 53BP2. In this study, we have examined the genomic organization of TP53BP2 transcripts and found that it encodes two mRNA species, either with (53BP2) or without exon 3 (ASPP2), by alternative splicing in various cell lines and tissues. Thus, we propose to call these proteins as 53BP2S (short) and 53BP2L (long), respectively.

Keywords: TP53BP2; 53BP2; ASPP 2; Apoptosis; p53; Alternative splicing

The p53 binding protein 2 (53BP2) has been initially identified as the interacting protein to p53 [1]. The 53BP2 protein consists of an open reading frame (ORF) of 1005 amino acids (aa) with α-helical region, proline-rich region, ankyrin repeats, and Src-homology 3 (SH3) domain [2]. The 53BP2 binding site on the p53 core domain consists of evolutionarily conserved regions that are frequently mutated in human cancer [1,3]. It has been demonstrated that overexpression of 53BP2 induced apoptosis [4–6] and that the level of 53BP2 mRNA expression in various human cancer cell lines was correlated with the sensitivity to DNA damaging agents such as UV irradiation, X-ray irradiation, and *cis*-diamine-dichloroplatinum (CDDP) [7]. 53BP2 has also been shown to interact with Bcl-2 [2] and nuclear factor κB (NF-κB) p65 subunit [6]. Because of its interaction with these proteins, 53BP2 is implicated in carcinogenesis. A recent report by Samuels-Lev et al. [10] has revealed the presence of longer ORF of 1128 aa containing the additional 123 aa to the N-terminus of 53BP2 [thus, they renamed this protein as ASPP2 (apoptosis stimulating protein of p53 2)] and claimed that 53BP2 might be a partial clone of ASPP2 [8]. As we have previously reported that the TP53BP2 gene is a single copy gene and has been mapped on the long arm of chromosome 1 at q42.1 [9], the relationship between 53BP2 and ASPP2 has been elusive.

In this study, we have examined the genomic organization of the TP53BP2 gene (human genome locus ID: 7159; Accession No. NT_004559.11) encoding 53BP2 and ASPP2 proteins. The previously reported ORF of 53BP2 was derived from an actual cDNA clone isolated from a human cDNA library (Accession No. NM_005426) [2,6] and that of ASPP2 (Accession No. AJ318888) was identified by genome database search [10]. Here we demonstrate the evidence that 53BP2 is not a partial and truncated form of ASPP2 and endogenous 53BP2, as well as ASPP2, is present in various cells and tissues. Thus, TP53BP2 encodes two mRNA species, either with (53BP2) or without exon 3 (ASPP2), by alternative splicing.

* Corresponding author. Fax: +81-52-859-1235.
E-mail address: tokamoto@med.nagoya-cu.ac.jp (T. Okamoto).

0006-291X/S - see front matter © 2004 Elsevier Inc. All rights reserved.
doi:10.1016/j.bbrc.2004.01.079